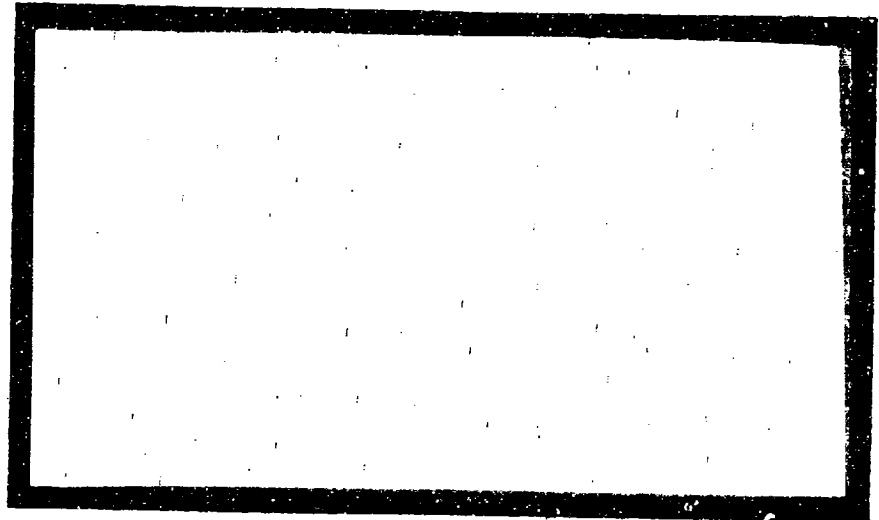


AD734676



DISTRIBUTION OF THIS DOCUMENT IS UNLIMITED

# Project THEMIS

CONTRACT ONR-N00014-68-A-0152

University of Notre Dame  
college of engineering  
notre dame, indiana

DDC  
RECEIVED  
JAN 6 1972  
B

46556  
DISTRIBUTION STATEMENT A  
Approved for public release;  
Distribution Unlimited

Reproduced by  
NATIONAL TECHNICAL  
INFORMATION SERVICE  
Springfield, Va. 22151

66

UNCLASSIFIED

Security Classification

## DOCUMENT CONTROL DATA - R&amp;D

(Security classification of title, body of abstract and indexing annotation must be entered when the overall report is classified)

1. ORIGINATING ACTIVITY (Corporate author) College of Engineering University of Notre Dame		2a. REPORT SECURITY CLASSIFICATION UNCLASSIFIED	
		2b. GROUP	
3. REPORT TITLE Drag Reduction Degradation of Dilute Polymer Solutions in Turbulent Tube Flow			
4. DESCRIPTIVE NOTES (Type of report and inclusive dates) Technical Note			
5. AUTHOR(S) (Last name, first name, initial) Sylvester, Nicholas D. and Kumor, Stanley M.			
6. REPORT DATE November 1971	7a. TOTAL NO. OF PAGES 55	7b. NO. OF REFS 77	
8a. CONTRACT OR GRANT NO. ONR-N00014-68-A-0152	8b. ORIGINATOR'S REPORT NUMBER(S) UND 71-6		
b. PROJECT NO. In House Account No. UND 99850	9b. OTHER REPORT NO(S) (Any other numbers that may be assigned this report)		
c.			
d.			
10. AVAILABILITY/LIMITATION NOTICES Document cleared for public release and sale; its distribution is unlimited			
11. SUPPLEMENTARY NOTES		12. SPONSORING MILITARY ACTIVITY Department of the Navy Office of Naval Research	
13. ABSTRACT Drag reduction degradation characteristics of Separan AP30 are reported in this work. A recycle tube flow experiment was used to investigate this property of drag reducing polymer solutions. Experimental pressure gradient and flow rate measurements were made as a function of time. From this data, friction factor-time plots on log-log coordinates were constructed, all of which exhibited three distinct regions: <ol style="list-style-type: none"> <li>1. At short times, a constant friction factor given by Virk's maximum drag reduction equation.</li> <li>2. A Linear region in which the friction factor increases with time for time greater than <math>\theta_D</math>.</li> <li>3. At long times, an asymptotic nonlinear approach of the polymer solution friction factor toward the solvent friction factor.</li> </ol> Correlations are presented relating $\theta_D$ the process time maximum drag reduction exists, and $\theta_E$ the process time significant drag reduction exists ( $20 \pm 5\%$ ) to the polymeric and system flow variables. Correlation are also presented relating $\theta_D$ , the real time maximum drag reduction exists for a solution under continuous turbulent flow, and $\theta_E$ , the real time significant drag reduction exists for a solution under continuous turbulent flow, to variables of primary interest; intrinsic viscosity, concentration, and velocity. Although the correlations are limited to the range of variables studied, the essential features of the drag-reduction degradation behavior of dilute polymer solutions in turbulent tube flow have been demonstrated.			

DD FORM 1 JAN 64 1473

UNCLASSIFIED

Security Classification

DRAG REDUCTION DEGRADATION OF DILUTE  
POLYMER SOLUTIONS IN TURBULENT TUBE FLOW

by

Nicholas D. Sylvester and Stanley M. Kumor

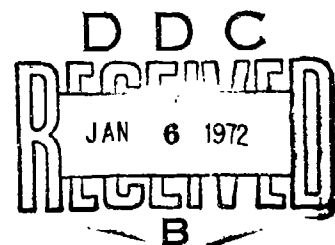
November, 1971

Document cleared for public release and sale:

Distribution is unlimited.

Project THEMIS  
University of Notre Dame  
College of Engineering  
Notre Dame, Indiana 46556

Contract  
N00014-68-A-0152(NR 260-112/7-13-67)



TECHNICAL REPORT  
NUMBER:  
THEMIS-UND-71-6

DISTRIBUTION STATEMENT A

Approved for public release;  
Distribution Unlimited

UNCLASSIFIED

Security Classification

KEY WORDS	LINK A		LINK B		LINK C	
	ROLE	WT	ROLE	WT	ROLE	WT
Drag Reduction Turbulent Flow Macromolecular Degradation Dilute Polymer Solutions						

DD FORM 1 NOV 61 1473 (BACK)

101-507-6-21

UNCLASSIFIED

Security Classification

A-11409

## FOREWORD

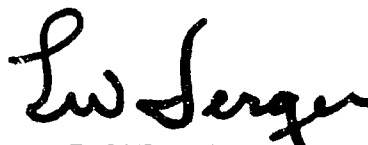
This technical report was prepared by the Thermal Systems Group under Project THEMIS at the University of Notre Dame, College of Engineering. The co-authors, Dr. Nicholas D. Sylvester and Mr. Stanley M. Kumor are respectively Assistant Professor and Research Assistant in the Chemical Engineering Department.


The research was performed under the sponsorship of the Department of the Navy, Office of Naval Research, Washington, D. C. 20360, with funding under Contract N00014-68-A-0152 and In-House Account Number UND-99850.

The authors wish to express their appreciation to Mrs. Helen Deranek for her careful typing of the manuscript and to Professor Hugh P. Ackert for the preparation of the illustrations.

Readers are advised that reproduction in whole or in part is permitted for any purpose of the United States Government.

This technical report has been reviewed and approved for submittal to the sponsoring agency November, 1971.

  
EDWARD W. JERGER  
Program Manager  
Project THEMIS

  
JOSEPH C. HOGAN  
Dean, College of Engineering  
University of Notre Dame

ABSTRACT

Drag reduction degradation characteristics of Separan AP30 are reported in this work. A recycle tube flow experiment was used to investigate this property of drag reducing polymer solutions. Experimental pressure gradient and flow rate measurements were made as a function of time. From this data, friction factor-time plots on log-log coordinates were constructed, all of which exhibited three distinct regions:

1. At short times, a constant friction factor given by Virk's maximum drag reduction equation.
2. A linear region in which the friction factor increases with time for time greater than  $\theta_D$ .
3. At long times, an asymptotic nonlinear approach of the polymer solution friction factor toward the solvent friction factor.

Correlations are presented relating  $\theta_D$ , the process time maximum drag reduction exists, and  $\theta_E$ , the process time significant drag reduction exists ( $20 \pm 5\%$ ) to the polymeric and system flow variables. Correlations are also presented relating  $\theta_D'$ , the real time maximum drag reduction exists for a solution under continuous turbulent flow, and  $\theta_E'$ , the real time significant drag reduction exists for a solution under continuous turbulent flow, to variables of primary interest: intrinsic viscosity, concentration, and velocity. Although the correlations are limited to the range of variables studied, the essential features of the drag-reduction degradation behavior of dilute polymer solutions in turbulent tube flow have been demonstrated.

TABLE OF CONTENTS

	<u>Page</u>
1. Introduction	1
2. Previous Studies	5
3. Apparatus	13
4. Experimental Procedure	18
5. Results and Discussion	20
a) Polymer and Dilute Solution Properties	20
b) Drag Reduction and Drag Reduction Degradation	24
c) Analysis and Correlation of $\theta_D$ and $\theta_E$	29
6. Conclusions and Recommendations	45
7. Bibliography	48
8. Appendix	52

List of Tables

	<u>Page</u>
1. Legend of Experimental Apparatus	15
2. List of Intrinsic Viscosity Values for Polymer Solutions Studied.	22
3. Analysis of the Treated Water Used in the Experiments.	23
A1. Summary of the SAP30 Drag Reduction Degradation Data	54-55



List of Figures

	<u>Page</u>
1. Schematic of Experimental Apparatus.	14
2. Comparison of solvent friction factor-Reynolds number data with the Blasius equations.	17
3. Reduced viscosity-concentration plots for all Separan-solvent systems tested.	21
4. Friction factor-time plot for representative polymer solutions.	26
5. Friction factor-Reynolds number plot for all the polymer solutions tested.	27
6. Percent drag reduction-time plot for various polymer concentrations at various velocities.	30
7. $\theta_D$ versus solution volume tested.	32
8. $\theta_D$ versus length of flow section used.	33
9. $\theta_D$ versus flow velocity.	34
10. $\theta_D$ versus polymer concentration.	35
11. $\theta_D$ versus intrinsic viscosity.	36
12. $\theta_D$ versus X plot for all polymer solutions tested.	39
13. $\theta_E$ versus X plot for all polymer solutions tested.	40
14. $\theta'_D$ versus Y plot for all polymer solutions.	42
15. $\theta'_E$ versus Y plot for all polymer solutions.	43

NOMENCLATURE

C	Polymer concentration (gm/dl)
$\frac{dP}{dx}$	Pressure gradient $\frac{\text{dynes}}{\text{cm}^2}$
EFF Vol <sub>system</sub>	Effective volume of test section
$f_p$	Friction factor of polymer solution
$f_s$	Friction factor of solvent
$K_D$	Constant defined by Eq. (8)
$K'_D$	Constant defined by Eq. (10)
$K_E$	Constant defined by Eq. (9)
$K'_E$	Constant defined by Eq. (11)
L	Length of test section (cm)
L'	Equivalent length of pump (cm), given by Eq. (A-4)
Q	Volumetric flow rate (cm <sup>3</sup> /sec)
R	Tube radius (cm)
Re <sub>s</sub>	Solvent Reynolds number
V	Spatial average velocity (cm/sec)
V <sub>Sol</sub>	Solution volume tested (cm <sup>3</sup> )
X	Variable defined by Eq. (7)
Y	Variable defined by Eq. (12)

NOMENCLATURE (continued)

$[\eta]$	Intrinsic viscosity (dl/gm)
$\eta_{sp}$	Specific viscosity
$\rho$	Fluid density (gm/cm <sup>3</sup> )
$\theta_D$	Process time maximum drag reduction exists (min)
$\theta'_D$	Real time maximum drag reduction exists for solution under continuous shear. (sec)
$\theta_E$	Process time significant drag reduction exists (20 $\pm$ 5%) (min)
$\theta'_E$	Real time significant drag reduction exists for solution under continuous shear (min)
$\mu$	Solvent viscosity (gm/cm.sec)

Acknowledgements

The authors are grateful for the assistance of Bill Hassink, Pat Shuler, and James Tyler in carrying out some of the experimental work, and to the Dow Chemical Company for supplying the Separan AP30. The authors thank the Department of the Navy (Office of Naval Research) and the Department of Chemical Engineering for their financial support.

Introduction

The phenomena of turbulent flow-drag reduction, which can be defined as an increase in the volumetric flow rate at a given pressure drop usually due to the addition of a linear, high molecular weight polymeric material to a low viscosity liquid, has received considerable attention because of the many applications of both theoretical and pragmatic interest. Drag reduction is well documented (see, for example, references, 1-10) and a recent review is available (11) which summarizes typical data and discusses many of the empirical and theoretical analyses that have appeared. The many experimental studies, as summarized by Virk (7) and expanded here, indicate the existence of three regimes of turbulent flow.

- a) A regime without drag reduction wherein the polymer solutions obey the same friction factor relation as the Newtonian solvent.
- b) A regime with drag reduction in which the friction factor relation obeyed by a given solution depends at least upon the following system parameters - the polymer-solvent, polymer molecular weight, molecular weight distribution, concentration, tube diameter, and turbulent flow time. The onset of drag reduction, i.e. the demarcation between regimes (a) and (b), is usually well defined.
- c) An asymptotic regime which ultimately limits the maximum drag reduction possible. The friction factor relation for this ultimate asymptote appears to be independent of polymer parameters.

Although a number of theoretical models have been proposed (see for example, reference 5,6,7,12-19), the mechanism of drag reduction is still obscure; however, the following observations appear to be significant. The phenomenon results from some kind of interaction between the polymer molecules and the turbulent flow field. The polymer-turbulence interaction, however, it occurs, markedly affects the region close to the tube wall. The phenomenon depends strongly on the concentration of the highest molecular weight species present in the molecular weight distribution and appears to exist in the limit of infinite dilution. The above observations have been discussed in detail by Virk (7) and Paterson and Abernathy (10) and imply that it is in the buffer zone, of known importance in the energetics of turbulent flow (20-25), that the polymer-turbulence interaction responsible for drag reduction occurs.

A number of experimental investigations (see, for example, references 9,10,26-54) have shown that any high shear field (e.g. the turbulent flow field) can cause polymer degradation (rupture of covalent molecular bonds due to severe deformation resulting in molecular scission) manifesting itself as a decrease in polymer molecular weight and drag reduction effectiveness with time of shear. This degradation (chain breakage) may impose severe limitations on uses whose effectiveness is controlled by the very high molecular weight molecules which have been shown to be more sensitive to high shear (10,45,50,51,54-57). This type of problem has been encountered in such practical applications as viscosity index improvement of lubricating oils (29,58-63) and drag reduction (9,10,33,34,54). It also impairs the reliability of rheological characterization at high shear (64) and molecular weight determination by Gel Permeation Chromatography (10).

The studies to be discussed below show that polymer degradation under high shear is severe, that the highest molecular weight polymeric materials are preferentially attacked and that, in reference to turbulent flow-drag reduction, the most likely mechanism is, in the absence of chemical reactions, a hydrodynamic interaction between the polymer molecules and the turbulent flow field.

One way to monitor polymer degradation and at the same time evaluate the drag reduction effectiveness of a given polymer solution is to measure the solution friction factor as a function of the time of flow. In this study, the effect of various independent variables (polymer concentration, polymer solution intrinsic viscosity, and flow velocity) on turbulent flow drag-reduction degradation was investigated. The ranges of the variables studied was limited to those shown below by the experimental equipment available. The polymer studied was Separan AP30 (SAP30, Dow Chemical) a partially hydrolyzed polyacrylamide (71).

1. Polymer concentration:  $50 \leq C \leq 200$  wppm
2. Intrinsic viscosity:  $12 \leq [\eta] \leq 132$  dl/g
3. Flow velocity:  $140 \leq V \leq 410$  cm/sec which gave a solvent Reynolds number range of 10,500 to 31,000.

In addition to these independent variables the effects of feed solution volume (25-50 liters) and flow system length were determined (7-51 feet). Not including tube diameter, which was not varied, there are five independent variables; thus, most of the experimental data is confined to aqueous SAP30 solutions having an intrinsic viscosity of 41.0 dl/g.

Correlations for the real flow time under continuous, turbulent tube flow ( $\theta'_D$ ) that maximum drag reduction will exist and the real flow time under continuous, turbulent tube flow ( $\theta'_E$ ) that significant drag reduction (approximately 20% or more) will last have been determined. The correlations of both  $\theta'_D$  and  $\theta'_E$  are of the form

$$\theta' = KY$$

where  $Y = c^2 [\eta]^{3/2} / v^2$

and  $K = 10.92 \times 10^{-7} \frac{\text{cm}^2}{\text{sec}} \left( \frac{dl}{g} \right)^{1/2}$  for  $\theta'_D$  in seconds

$$K = 6.6 \times 10^{-7} \frac{\text{min.cm}^2}{\text{sec}^2} \left( \frac{dl}{g} \right)^{1/2} \text{ for } \theta'_E \text{ in minutes}$$

The correlations presented are, of course, limited to the range of variables studied; however, it is believed that the essential drag-reduction degradation behavior of dilute polymer solutions in turbulent flow has been demonstrated and that the ideas and results presented should stimulate additional research which will further elucidate this highly complex and important phenomena.



Previous Studies

An understanding of the process of turbulent flow degradation of high molecular weight materials is essential to the interpretation of drag reduction measurements, to the determination of the true dependence of drag reduction on polymer concentration and molecular weight, and to the selection of the most suitable drag-reducing polymer for a given application.

The phenomenon of polymer degradation has been under investigation for more than three decades and although many excellent papers have been published, complete understanding is lacking because of the multiplicity of factors which can contribute to the molecular scission. Polymer molecules can be degraded by both mechanical and chemical means and turbulent flow degradation may be some combination of the two, depending on the polymer solvent system. The interpretation of available results is complicated by the diverse experimental methods used to produce degradation and the number of different polymer-solvent systems studied. For simplicity, chemical and mechanical degradation will be discussed separately, although their interrelationships will be pointed out.

Polymeric hydrocarbons are subject to oxidation by atmospheric oxygen, and it is generally agreed that the oxidation reaction proceeds by a free radical, chain mechanism (65-67). The first step in an oxidative degradation reaction is the generation of a free radical on a polymer chain, which under normal conditions is extremely slow. These radicals can be formed by absorption of heat, ultraviolet light, high energy radiation, mechanical stress, and reaction with radicals from a foreign source. Once radicals have been generated within the polymer, rapid reaction with oxygen will occur forming peroxy radicals, if oxygen is available. Hydrogen abstraction

by the peroxy radicals leads to hydroperoxide formation. Although any carbon-hydrogen bond might provide the needed hydrogen, positions that are especially vulnerable are those adjacent to a double bond, adjacent to an ether linkage or on a tertiary carbon. Decomposition of hydroperoxides very often leads to chain scission. Various metal salts (e.g. ferrous, cuprous, cupric, and silver salts), which are often occluded in the polymer during polymerization, accelerate hydroperoxide decomposition, and are thus active oxidation catalysts. Metal ions may also catalyze the formation of oxygen free radicals capable of initiating degradation. Complete details can be found in references (65-67).

White (34) has presented preliminary experimental data on the degradation of poly(ethylene oxide) in turbulent flow which shows that the degradation rates are very rapid and that significant degradation can take place in a matter of seconds. White concludes that the degradation process is likely to be due to a direct oxidation step initiated by high frequency turbulent eddies. This interpretation is doubtful because the size of the smallest eddies is much greater than the polymer molecules; thus any collisions would be primarily elastic resulting in very little shear deformation.

Mechanical degradation will be discussed, for convenience, in two parts - ultrasonic degradation and shear degradation - although, in both cases, the polymer chain bonds in effect are broken as a result of physical stress.

Mechanical degradation induced by ultrasonic irradiation has been studied by many workers (e.g. references 45, 47-53, 55). Weissler (53) found that cavitation (the formation and violent collapse of small bubbles

in solution as a result of pressure changes which occur, for example, upon ultrasonic irradiation) was responsible for polymer degradation induced by ultrasonic irradiation in both polystyrene-toluene and hydroxyethyl cellulose-water systems. Gooberman (55) and Gooberman and Lamb (51) proposed and tested a mechanism for ultrasonic degradation of very dilute solutions based on the assumption that the degradation is due to the stresses set up within a macromolecule adjacent to a collapsed cavity and the stresses set up are due to the shock wave radiated from the cavity. This shock wave was pictured as a rapid pressure rise followed by a sharp exponential pressure drop (68). During the pressure drop, entrained solvent molecules will flow out of the macromolecule, and since their velocity relative to the macromolecule will increase with distance from its center of mass, a velocity gradient will be set up producing a stress which, if sufficiently great, will rupture a chemical bond. It was also assumed that the polymer solutions were dilute such that intermolecular interactions were negligible. The theory indicates that the higher the molecular weight of a given species, the more susceptible it is to scission, and the bond most likely to break will be one near the center of mass of the macromolecule, and a limiting molecular weight range should exist below which mechanical degradation should not occur. Experimental verification of the model was obtained for very dilute solutions (0.002%) of polystyrene in benzene. No degradation products of molecular weight less than about  $5 \times 10^4$  were detected. At concentrations greater than 0.01% the theory began to break down. This was attributed to intermolecular interactions which reduce the rate of cavity collapse. However, another possible explanation is the fact that cavitation intensity varies with solution viscosity which depends on concentration for a given

molecular weight and depends on molecular weight for a given concentration.

It can be concluded, from the many ultrasonic degradation studies, that mechanical stress is the primary mechanism of degradation even though some free radical attack will occur depending upon the polymer-solvent system studied (38,47,50,69); aqueous systems being most susceptible. The apparent discrepancies among various experimental studies (45,50) can in most cases be explained by the fact that all reported results are strongly dependent on experimental conditions.

Shear degradation will be discussed assuming cavitation to be absent, although bearing in mind that under suitable experimental conditions, it may occur and contribute to the observed degradation. Shear degradation has been studied under various high speed mixing conditions (35-44) and in laminar (30,54) and turbulent tube flow systems (9,10,33).

Nakano and Minoura (35,36) have studied the degradation of poly (ethylene oxide) and poly (methyl methacrylate) in benzene by high-speed stirring. The effects of polymer concentration, solvent, stirring speed, and initial degree of polymerization on the rate of scission were investigated. Their studies showed that in the concentration range, 1-4% w/v, degradation was not caused by the interaction of polymer chains, as did those of Arai and co-workers (41) and Harrington (43), and that a limiting molecular weight is generally observed. However, Grohn and Opitz (42) and Goto and Fujiwara (70) contend that interaction between polymer molecules plays an important role in shear degradation. Bueche (56) and Bestul (57) have presented theories postulating that the entanglements along the polymer chains play a major role in the rupture process for molten polymers when chemical reactions subsequent to chain rupture are neglected. General agreement between the theories and available experimental data (see references

1 and 2 of reference 56) is shown.

Two points can be made in an attempt to partially resolve these apparently contradictory results. As the concentration of a solution of a polymer of given molecular weight increases, the probability of entanglements between chains increases as does the viscosity of the solution. Similarly, the probability of entanglements increases as polymer molecular weight increases for a given concentration. Since shear degradation occurs in the limit of infinite dilution (9,10,33,51), the interaction between solvent and polymer chains brings about scission and entanglements of polymer chains are not necessary; although, their effect, if any, may not be observable if only a limited concentration range is studied. Ignoring the effect of chemical reactions may further complicate the interpretation of experimental data. Also, the experimental work referred to by Bueche was for undiluted polymers where entanglements are expected to be a primary factor. Thus the effect of entanglements will depend on at least the polymer-solvent system, the polymer concentration, polymer molecular weight and the polymer conformation in solution.

Ram and Kadim (30) studied the shear degradation of polyisobutylene solutions in laminar flow through capillaries. The effects of initial molecular weight, concentration, temperature, and wall shear stress on degradation were investigated. They found that the apparent viscosity of a given polymer solutions (measured under low stress conditions) decreased with time of shearing at high stresses and approached an asymptotic value and that the magnitude of the value decreased as the shear stress increased. It was also found that for a constant shear stress degradation was less effective (in terms of the relative drop in average molecular weight) as

polymer concentration increased in contrast to other published results. This discrepancy can be explained by the following argument. To maintain shear stress constant for a given tube while increasing polymer concentration, it is necessary to decrease the flow rate and thus decrease the shear rate. Since it is the shear field which controls the hydrodynamic forces on the polymer chains, the results of Ram and Kadim are expected and are indeed consistent with the results showing degradation increasing with increased concentration under constant shear rate conditions. In this case, when the concentration is increased with the shear rate held constant, the shearing stresses will be increased producing increased degradation.

Patterson et.al (54) studied the effect of degradation by pumping on normal stresses and drag reduction for polyisobutylene in toluene and cyclohexane. They found from molecular weight distribution curves and intrinsic viscosities that the major effect of mechanical degradation was the breakdown of the largest polymer molecules with a relatively small decrease in the viscosity-average molecular weight. They also found from drag reduction measurements that polyisobutylene degraded faster in toluene than in cyclohexane. Toluene is a better solvent (i.e. the polyisobutylene molecules are more expanded in toluene) than cyclohexane indicating that the interaction with solvent has a strong effect on degradation rates. However the use of turbulent flow drag reduction results to draw conclusions concerning the degradation characteristics of different polymer-solvent systems can be misleading, because the drag reduction characteristics themselves are strongly dependent on the polymer-solvent system. For example, the better the solvent for a given polymer, all other things being equal, the greater the drag reduction. Thus, as will be shown below, one must be

very careful indeed when analyzing turbulent flow drag reduction degradation data because of the coupled and highly nonlinear phenomena involved.

Fisher and Rodriguez (33), Paterson and Abernathy (10) and Keilis (9) have recently presented data on shear degradation and drag reduction of various polymer solutions in turbulent tube flow. In each study, it was shown that the decrease in drag reduction effectiveness due to degradation was very rapid and severe. The study of Paterson and Abernathy is particularly noteworthy. The authors attempted to determine the change in polymer molecular weight distribution as a function of time of flow. Although shear degradation also occurred in their Gel Permeation Chromatography columns, they were able to obtain very important results. Also, a number of the present authors previous, intuitive contentions and those to be presented in this report concerning the drag reduction and degradation phenomena were substantiated experimentally. These results are listed below.

1. Intrinsic viscosity, in general, failed to correlate the drag reduction for fixed concentration and flowrate.
2. Drag reduction is more dependent on the molecular weight distribution of a given polymer than on its average molecular weight as determined by intrinsic viscosity.
3. Drag reduction depends primarily on the highest molecular weight species in a given distribution.
4. Drag reduction and degradation appears to exist in the limit of infinite dilution indicating that both phenomena are due to the interaction of individual polymer molecules with solvent.
5. The rate of degradation increases with polymer molecule size.

6. The molecular weight dependence of degradation is not uniquely determined by the weight average molecular weight. It appears that once the high molecular weight components of the distribution have been preferentially degraded, the rate of degradation slows down.

It should be obvious, based on the above, that both the ultrasonic-mechanical and shear-mechanical degradation processes are essentially the same. They both result from hydrodynamic polymer-solvent interactions caused by violent shearing of the bulk solutions at the molecular level, which can be achieved by ultrasonic irradiation, high speed stirring, or laminar and turbulent tube flows.

It is clear that in the turbulent flow of drag reducing polymer solutions, molecular degradation caused by both chemical and mechanical factors occurs. It is believed that the primary cause of degradation is the hydrodynamic interaction of solvent and polymer which will be facilitated by entanglements. Of course, if free radicals are formed during the mechanical degradation process oxidation by dissolved oxygen, which is readily available in aqueous solution, will also occur. The existence, in most all cases, of a limiting molecular weight range below which essentially no further degradation takes place is very strong evidence in favor of the above. The apparent superiority of many polymers (see for example, 9, 33 and this work) over poly(ethylene oxide) still needs further examination.



Apparatus

In order to evaluate some of the parameters involved in drag reduction and drag reduction degradation, a simple recycle pressure drop experiment was constructed and is illustrated in Figure 1. The circled numbers on Figure 1 correspond to those listed in Table I - the legend for Figure 1. Solutions to be tested were placed in the feed tank which was a 15 gallon drum coated internally with an epoxy resin paint to inhibit corrosion. The solutions were pumped from the feed tank through the system to a collection reservoir by an ECO constant volume gear pump (Model 400, rated 3 gpm) constructed of 304 stainless steel with teflon gears and equipped with a Reeves Motordrive variable speed transmission (194-1750 RPM). The system fittings, valves, and tubing (0.244" I.D.) were also constructed from 304 stainless steel. The collection reservoir was a 2" I.D. Pyrex glass pipe equipped with a three way Pyrex glass valve which allowed the solutions to be either returned to the feed tank or diverted through the sample part for flowrate measurements. Pressure drop measurements were made with 60" Meriam vertical monometers (Model 30 PA 10TM) connected to pressure taps located 10 ft. and 15 ft. from the end of the tube. The temperature for all runs was maintained at  $30.0^{\circ}\text{C} \pm 0.10^{\circ}\text{C}$  by a Sargent Thermometer (Model S). The feed tank was equipped with a cooling coil and a Lightening mixer (Model XP) with a 2-1/2" Propeller to insure that the solutions were adequately mixed.

The pressure drop apparatus was checked with water by comparing the experimentally determined friction factor with that calculated from the Blasius equation

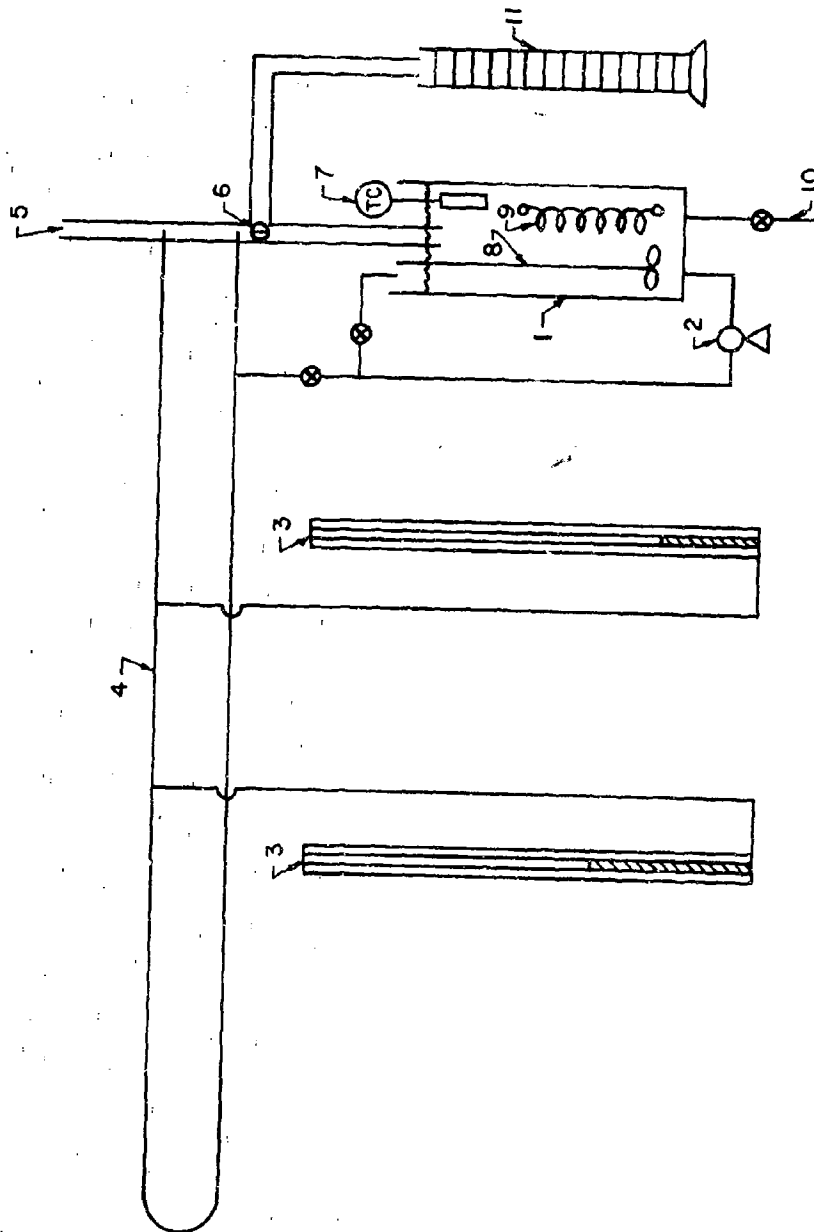


FIG. 1. Schematic of Experimental Apparatus

TABLE I

## Legend of Experimental Apparatus

1. Feed tank (capacity 15 gals)
2. Eco gear pump (Model 400) and Reeves motodrive variable speed transmission (194-1750 RPM).
3. Meriam 60" vertical manometer (Model 30 PA10TM).
4. Test section 3/8" O.D. S.S. 304 tubing 0.244" I.D.
5. Collection reservoir.
6. Sample port (3 way valve).
7. Sargent thermometer temperature controller (Model S).
8. Lightening mixer (Model XP).
9. Cooling coil.
10. Drain.
11. Sample vessel (2000 ML graduate cylinder).

$$f = 0.0791 (N_{RE})^{-1/4}$$

and the Prandtl-Karman law

$$\frac{1}{\sqrt{f}} = 4.0 \log_{10} (N_{RE} \sqrt{f}) - 4.0$$

The comparison with the Blasius equation is shown in Figure 2. The maximum deviation was - 3.60% and the average deviation was + 1.29% when compared to Blasius equation.

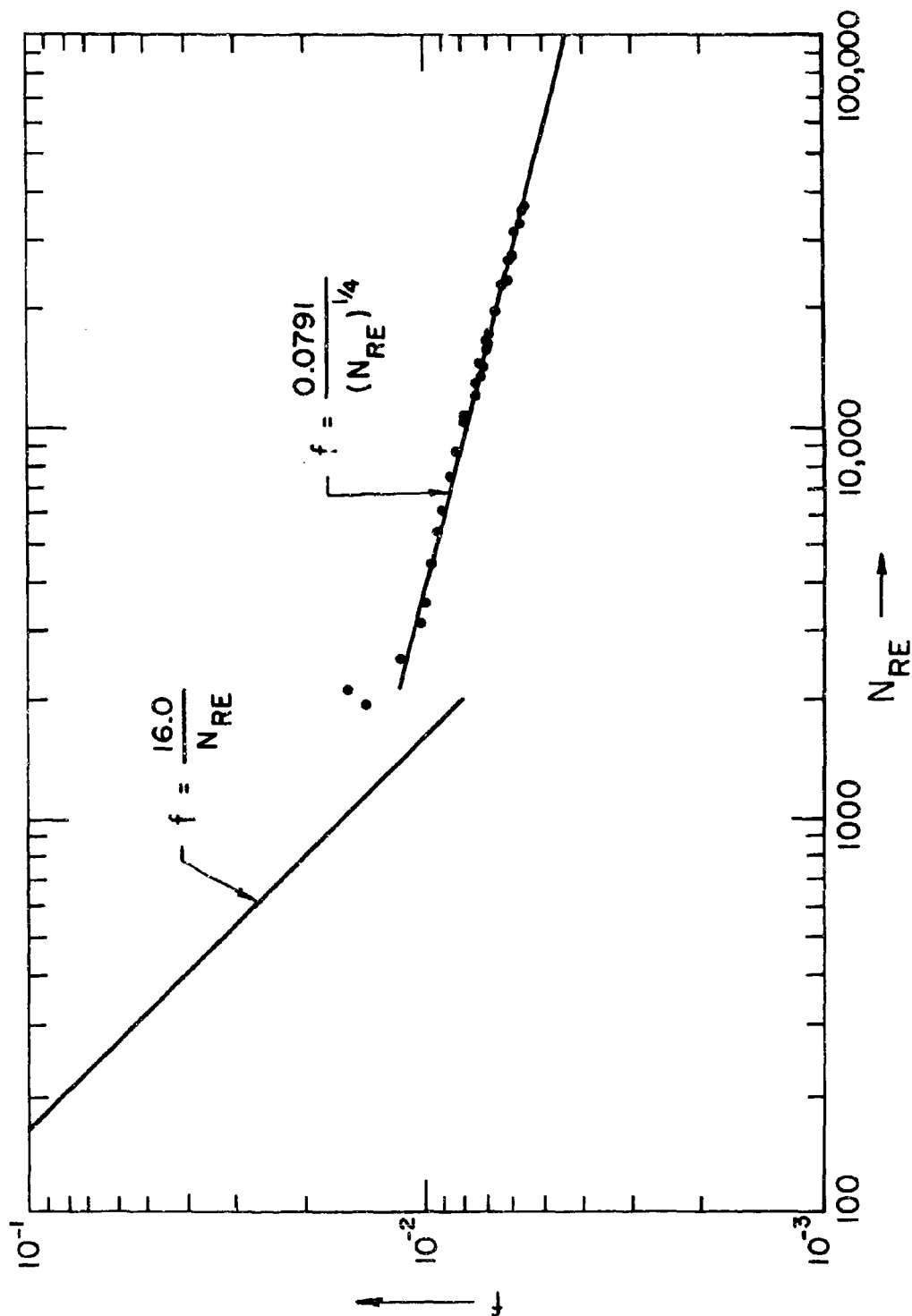


Fig. 2. Comparison of solvent friction factor-Reynolds number data with the Blasius equations.

Experimental Procedure

The drag reduction and drag reduction degradation experiments were conducted in the following manner.

On the day before an experiment, a concentrated solution of polymer was prepared such that when diluted in the feed tank the desired concentration was achieved. This method was used rather than preparing a master batch from which all experiments were run in order to avoid degradation of the polymer solution due to storage over long periods of time.

On the day of an experiment, the feed tank was filled with the amount of solvent required to give the desired polymer concentration. The mixer was started and the temperature controller turned on. Next, the pump was started and set to give the desired flowrate. The manometers lines were bled to insure that they were filled with liquid. The liquid bled from the manometer lines was measured and replaced with fresh solvent. This was done to avoid the possibility of residual polymer in the lines from previous runs. When the water had reached the desired temperature, the pressure drops and flowrates were measured twice. The flowrate was determined by diverting the flow of the collection reservoir through the sample part to the sample vessel for a given period of time and then weighing the contents of the sample vessel. Using the experimental values of the pressure drops and flowrates, the friction factors were calculated and compared to the value predicted by the Blasius equation. Typical agreement was  $\pm 2\%$ . This was done before each run to insure that the equipment was operating properly. Satisfied that the system was operating properly; the concentrated polymer solution was added to the feed tank and the timer started. Pressure drop and flowrate measurements were usually made at the following times:

## TIME (Min.)

0.5

1.0

2.5

5 - 60 (5 minute intervals)

60 - 120 (15 minute intervals)

120 - 240 (30 minute intervals)

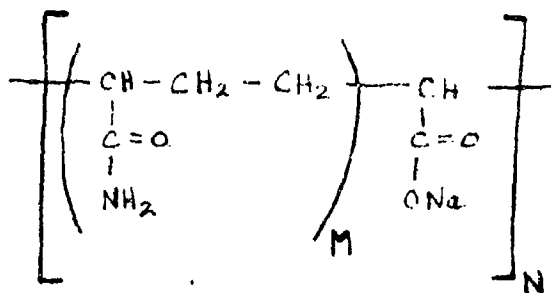
240 - (60 minute intervals)

At the conclusion of an experiment, the system was flushed with water at least twice and the manometer lines were bled. Experimental data were taken for nominal tube lengths of 51, 32, and 7 feet and feed solution volumes of 50, 37.5 and 25 liters. Data for a system length of 7 feet were taken by diverting the flow through the by-pass rather than the system. Pressure drop and flowrate measurements were taken at 30 minute intervals at which time the solution was run through the entire system for one minute to allow the manometers to come to equilibrium. The pressure drop and flowrate were recorded and the system again returned to by-pass operation.

Viscosity samples were taken for many runs at the following times: (0, 15, 30, 60, 120, 240, 480 minutes). After the first hour of a run relative viscosity measurements were made using a Fish-Schurman Ubbelohde viscometer (Model O<sub>o</sub> 003 - U - 304) suspended in a constant temperature bath. The temperature of the bath was maintained at  $30.0^{\circ}\text{C} \pm 0.001^{\circ}\text{C}$  by a Sargent Thermometer (Model S). This same viscometer assembly was also used to determine the intrinsic viscosity of all polymer-solvent systems tested.

Results and DiscussionPolymer and Dilute Solution Properties

The dilute solution properties of the drag reducing polymer studied here [Separan AP30 (Dow Chemical Co.) a partially hydrolyzed polyacrylamide], have been investigated by Sylvester and Tyler (71). The chemical structure of this flexible, high molecular weight, linear polymer can be represented by



where  $M \approx 3$  and  $N$  is large. The average molecular weight of this anionic polyelectrolyte is approximately two million. Polyelectrolytes are much more extended in solution because of the electrostatic repulsion of the chain ionic groups which leads to much higher intrinsic viscosity values (71).

The reduced viscosity-concentration data for Separan AP30 in various solvents is shown in Figure 3 and the intrinsic viscosity values are recorded in Table 2. An analysis of the treated water is given in Table 3. It is readily seen that the intrinsic viscosity of an aqueous-Separan AP30 solution is strongly dependent on the ionic content of the solvent. This type of behavior is well known for polyelectrolytes in general (72-74) and Separan AP30 in particular (71). As will be shown, the intrinsic viscosity of a polymer solution has a large effect on its drag reduction degradation characteristics.



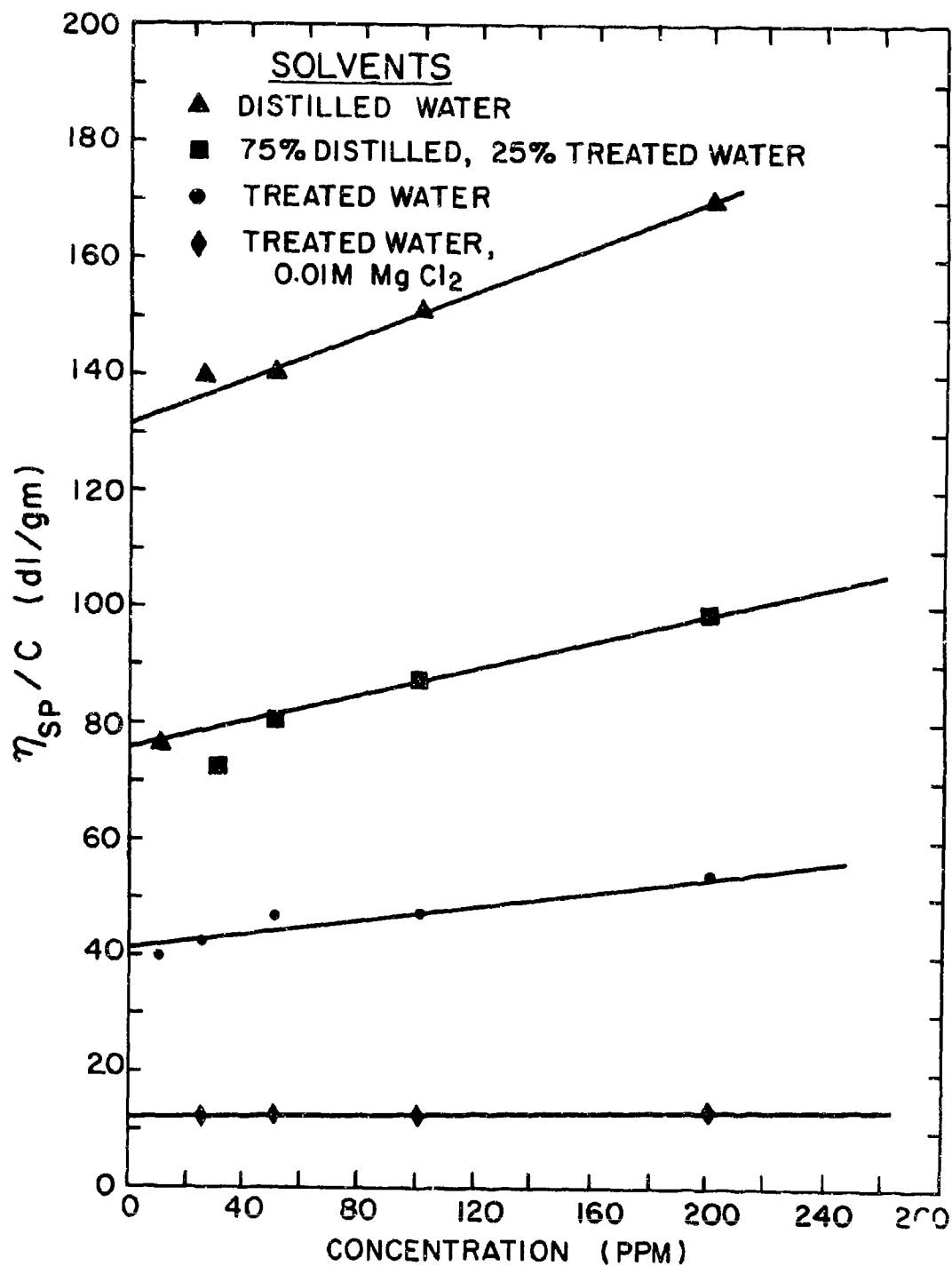


Fig. 3. Reduced viscosity-concentration plots for all Separan-solvent systems tested.

TABLE 2

Solvent	$[\eta]$	dl/gm
1. Distilled water		132.0
2. 75% distilled water 25% treated water		75.0
3. Treated water		41.0
4. 0.01M $\text{MgCl}_2$ in treated water		12.0

TABLE 3

## Analysis of Treated Water

	<u>Parts per million</u>		<u>Parts per million</u>
Total Dis. Solids	480.	Chloride (NaCl)	40.
Total Hard. ( $\text{CaCO}_3$ )	11.	Sulfate ( $\text{Na}_2\text{SO}_4$ )	174.
Ca. Hard. ( $\text{CaCO}_3$ )	7.	Silica ( $\text{SiO}_2$ )	10.
Mg. Hard. ( $\text{CaCO}_3$ )	4.	Total Iron (Fe)	0.4
Total Alk. ( $\text{CaCO}_3$ )	248.	pH	7.7
Manganese as Mn	0.05		

## DRAG REDUCTION AND DRAG REDUCTION DEGRADATION

The addition of a high molecular weight linear polymer to a low viscosity liquid can cause a dramatic decrease in the required pressure gradient at a given flowrate (1-10). However, if the polymer solution is continuously sheared in turbulent flow, degradation of the macro-molecules eventually occurs, resulting in an increased pressure gradient requirement. This phenomena is demonstrated very vividly in the representative friction factor versus time curves shown in Figure 4. These curves were constructed from experimental flowrate and pressure gradient measurements taken at specified intervals of time using the recycle pressure drop apparatus diagrammed in Figure 1. The measured volumetric flowrates were used to calculate the spatial average velocity from Equation (1)

$$V = \frac{Q}{\pi R^2} \quad (1)$$

The measured pressure gradient and the spatial average velocity,  $V$ , were used to calculate the friction factor from Equation (2)

$$f = \frac{\frac{R}{2} \left| \frac{dP}{dx} \right|}{\frac{1}{2} \rho V^2} \quad (2)$$

Note that both  $V$  and  $f$  are functions of time due to the degradation of the polymer solutions. The solvent Reynolds number is given by Equation (3).

$$Re_s = \frac{2\rho VR}{\mu} \quad (3)$$

where  $\mu$  is the solvent viscosity.

All the measured friction factor versus time data when plotted on log-log coordinates exhibited three distinct regions as shown in Figure 4.

- 1) At short times, a constant friction factor given by Virk's maximum drag reduction equation (7).
- 2) A linear region in which the friction factor increases with time for time greater than  $\theta_D$ .
- 3) At long times, an asymptotic nonlinear approach of the polymer solution friction factor toward the solvent friction factor.

For turbulent pipe flow of Newtonian fluids, the Blasius equation relates the friction factor and the Reynolds number and is given by Equation (4)

$$f = 0.0791 (Re_s)^{-0.25} \quad (4)$$

while the Virk equation, Equation 5, relates the minimum friction factor attainable with drag reducing polymer solutions to the solvent Reynolds number.

$$f = 0.59 (Re_s)^{-0.58} \quad (5)$$

Figure 5 shows the friction factor - Reynolds number data for all the solvents tested as well as the zero time friction factor - Reynolds number data for all Separan AP30 solutions tested. It can be seen that the solvent data is well represented by the Blasius equation and that at zero time all Separan solutions achieve maximum drag reduction as given by Virk.

For short times, the data points (see Fig. 4) fall on the maximum drag

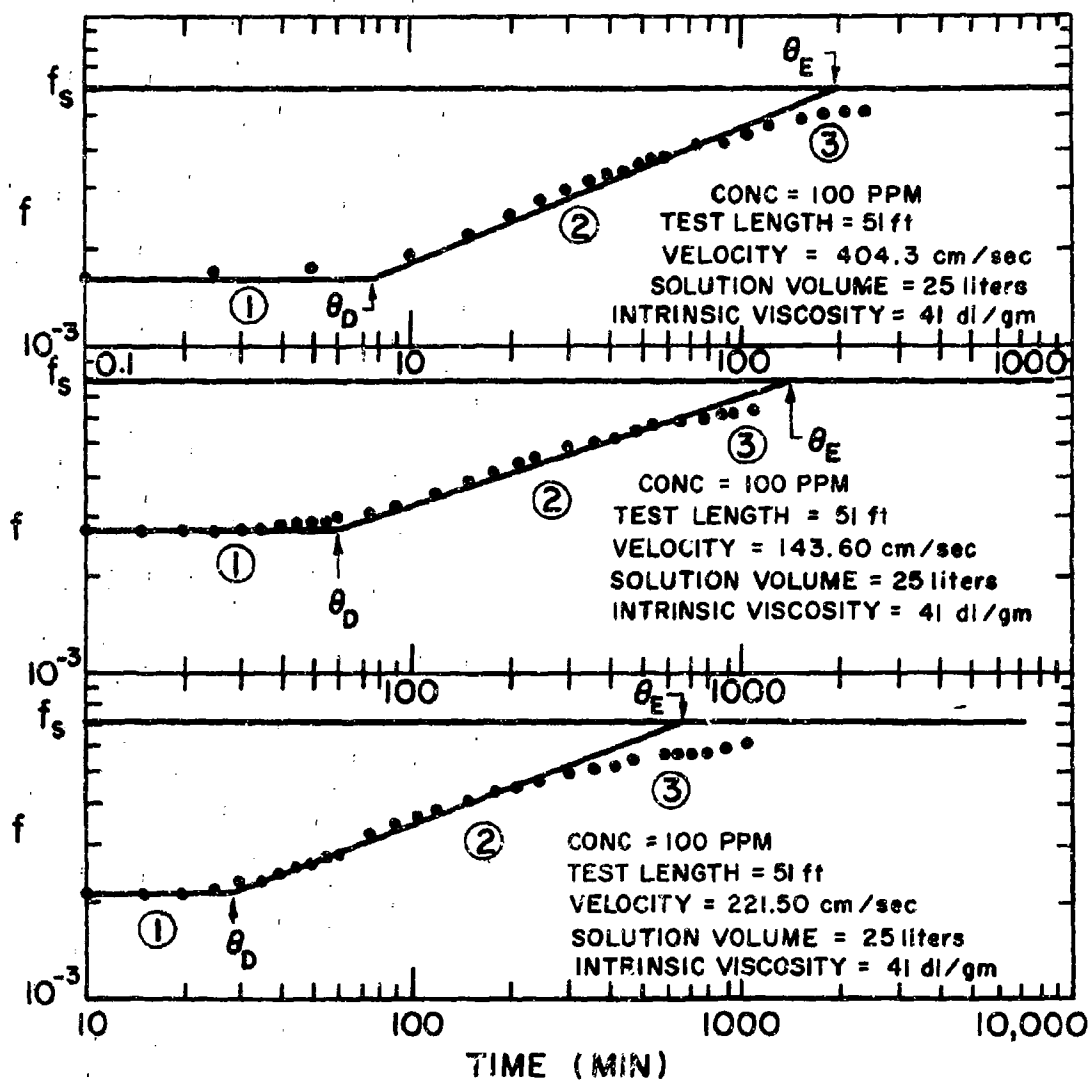


Fig. 4. Friction factor-time plot for representative polymer solutions.

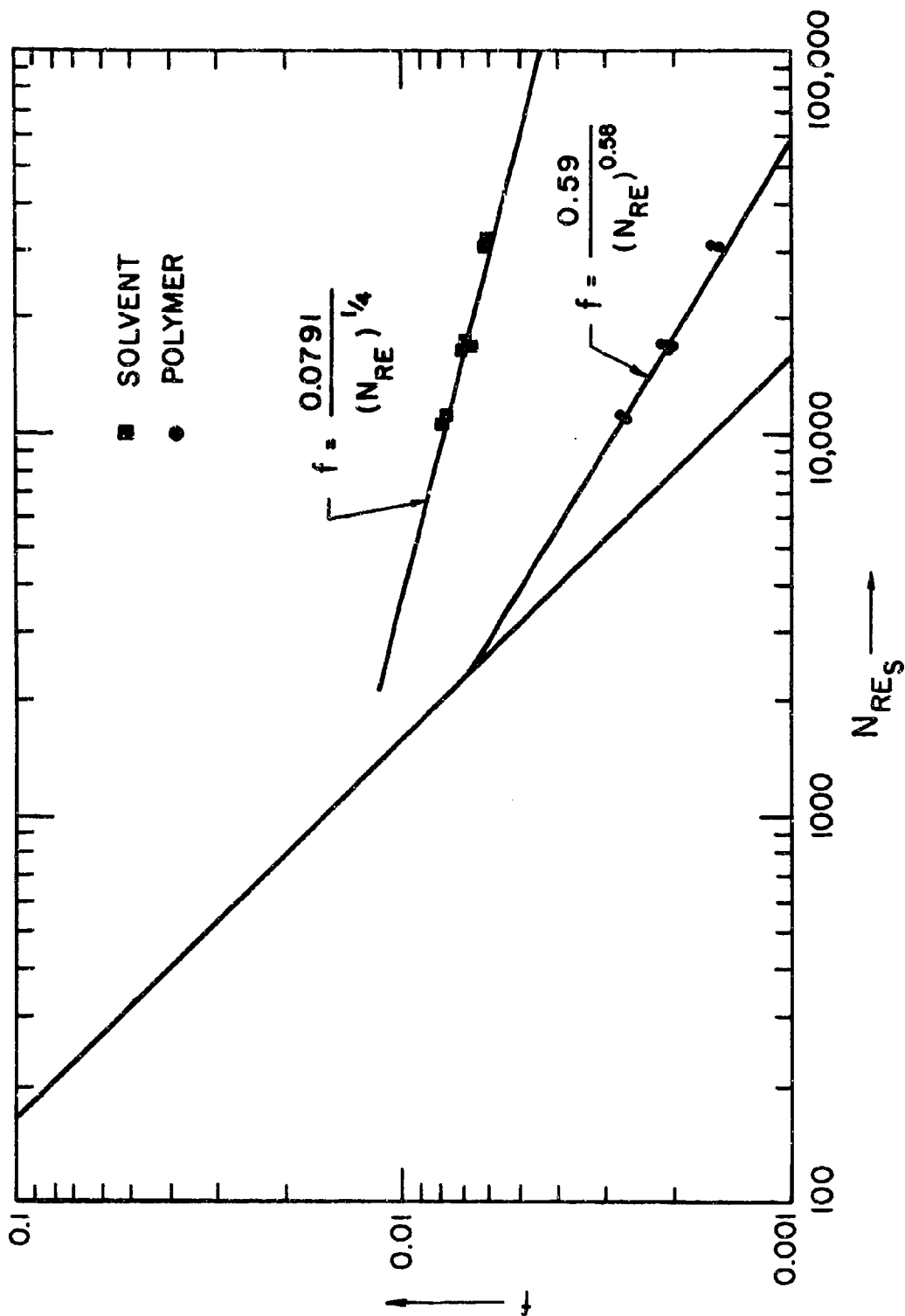


Fig. 5. Friction factor-Reynolds number plot for all the polymer solutions tested.

reduction asymptote; however, as time increases the solutions become progressively less effective in reducing frictional drag due to macromolecular degradation. During the constant friction factor period, degradation is definitely taking place but has not reached the extent where less than maximum drag reduction occurs.

On the basis of existing theory (55,56,57) and experiment (10,54), mechanical-shear degradation should preferentially attack the highest molecular weight components and the disproportionate decrease in drag reduction effectiveness depends primarily on the degradation of the highest molecular weight species of a polydisperse polymeric material. Thus solutions of higher concentration require longer flow times before the effect of degradation becomes noticeable. Above a certain concentration of high molecular weight components, the solution is saturated and maximum drag reduction is observed. As degradation attacks the higher molecular weight components the average molecular weight decreases but the observed drag reduction remains unaltered as long as their concentration remains above the minimum necessary for maximum drag reduction. As flow time and thus degradation proceed, the concentration of the drag reducing macromolecules continues to decrease ultimately becoming lower than the minimum required for maximum drag reduction and the measured friction factor begins to increase toward that of the solvent.

The time  $\theta_D$ , which is interpreted as the process time that a given polymer solution under a specific set of flow conditions will exhibit maximum drag reduction, was determined for all runs as the intersection of the extrapolated straight lines of regions one and two and is indicated in Figure 4. The time  $\theta_E$ , which is interpreted as the process time that a given polymer solution under a given set of flow conditions will exhibit



significant drag reduction (approximately  $20 \pm 5\%$ ) was determined for all runs as the intersection of the extrapolated straight lines of region two and the solvent friction factor and is also indicated in Figure 4. The times  $\theta_D$  and  $\theta_E$  have significant practical value for the design engineer. They will be correlated with polymeric and flow variables in this work to enable one to predict the drag reduction effectiveness of a given polymer solution under a specific set of turbulent flow conditions.

From the friction factor - time plots (see Figure 4) percent drag reduction versus time curves can be constructed. The percent drag reduction is given by Equation (6)

$$\% \text{ Drag Reduction} = \left[ 1 - \frac{f_p}{f_s} \right] \cdot 100 \quad (6)$$

where  $f_p$  is the friction factor of the polymer solution and  $f_s$  is the friction factor of the solvent at a given solvent Reynolds number.

Drag reduction histories for three polymer concentrations at each of three spatial average velocities are shown in Figure 6. It is seen that for a specific concentration the time maximum drag reduction is maintained increases with decreasing velocity and that for a given velocity the maximum drag reduction time increases with increasing concentration.

#### Analysis and Correlation of $\theta_D$ and $\theta_E$

The following experimental variables affected both  $\theta_D$  and  $\theta_E$  in a similar manner.

- a) Polymer solution volume.
- b) Length of the flow section including the pump.

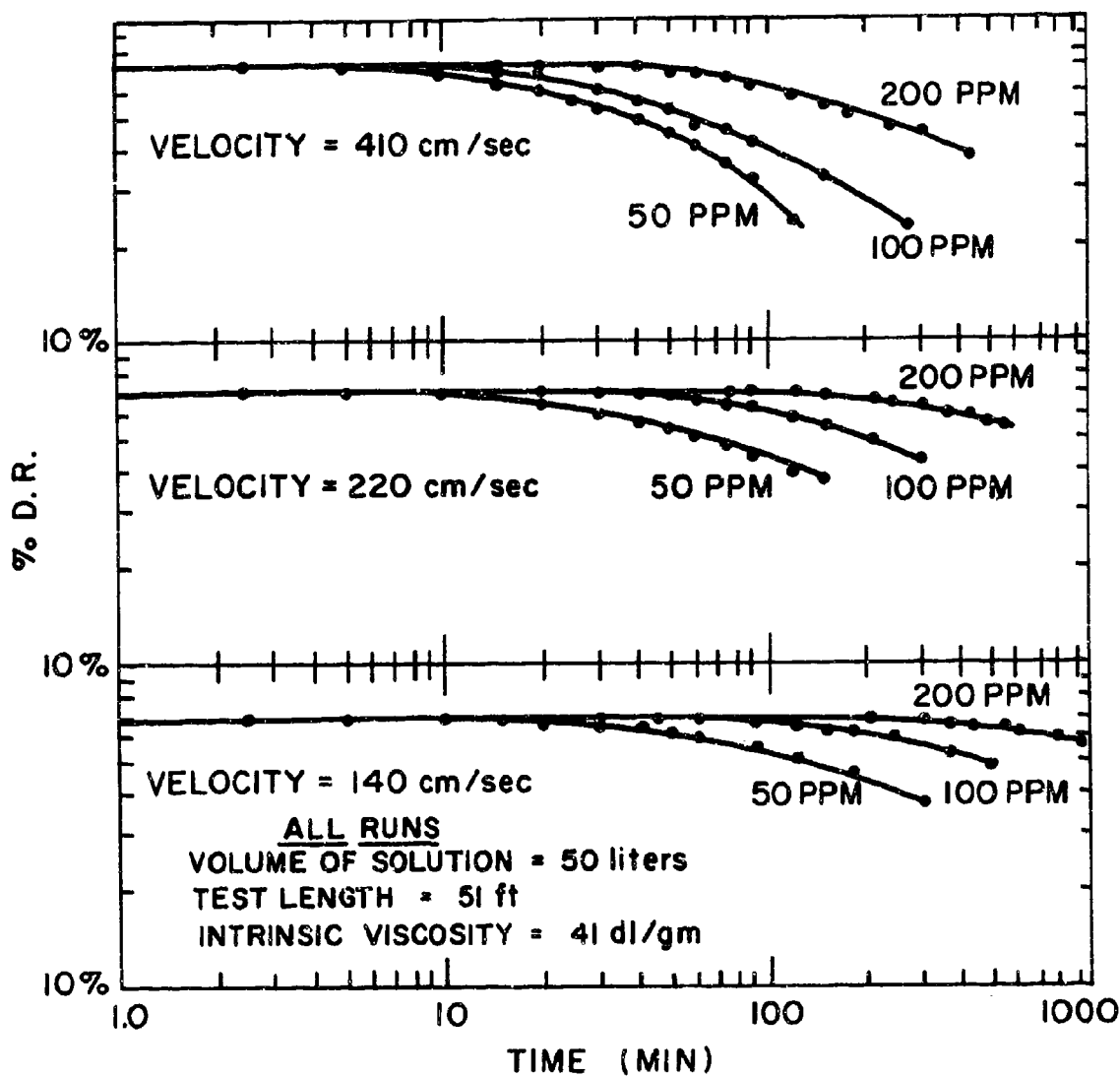
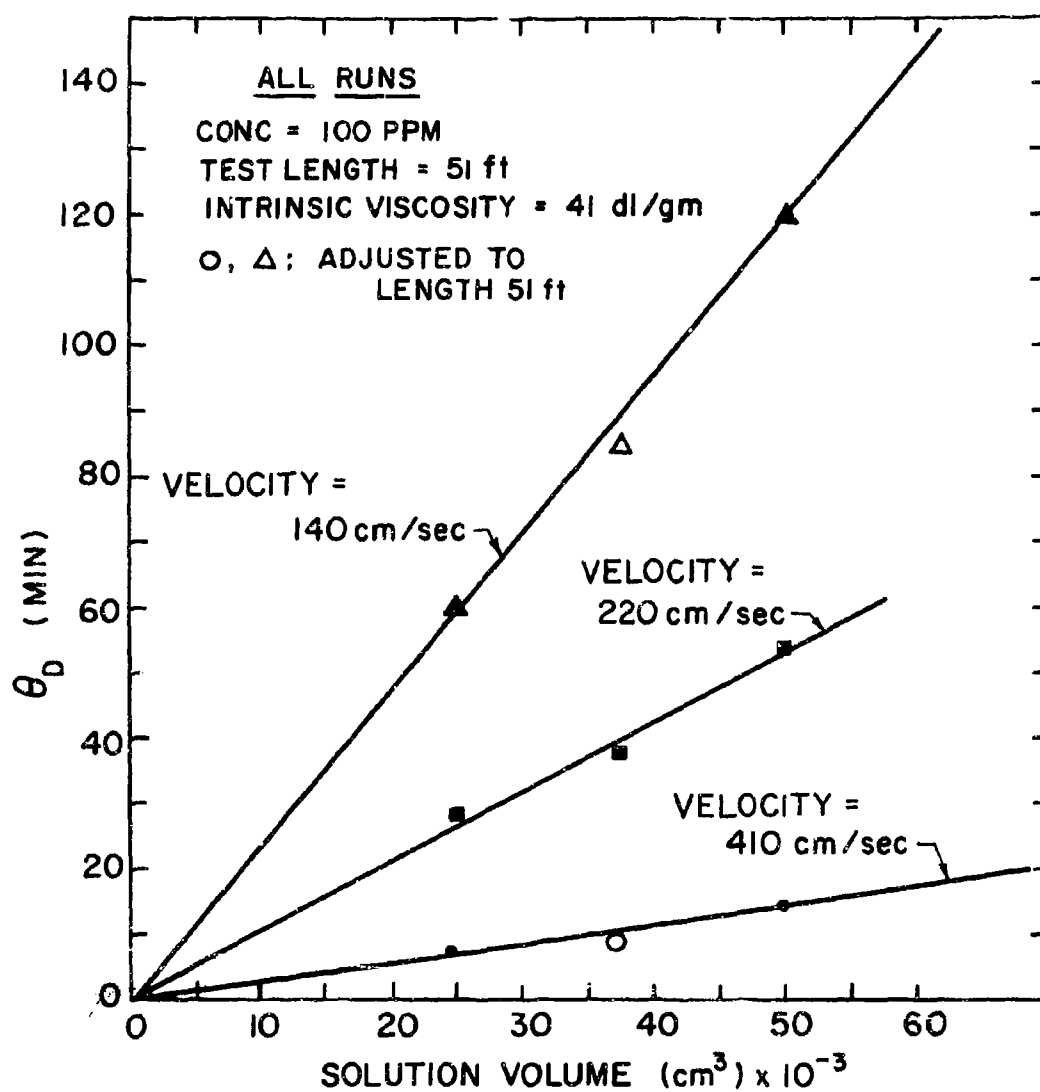


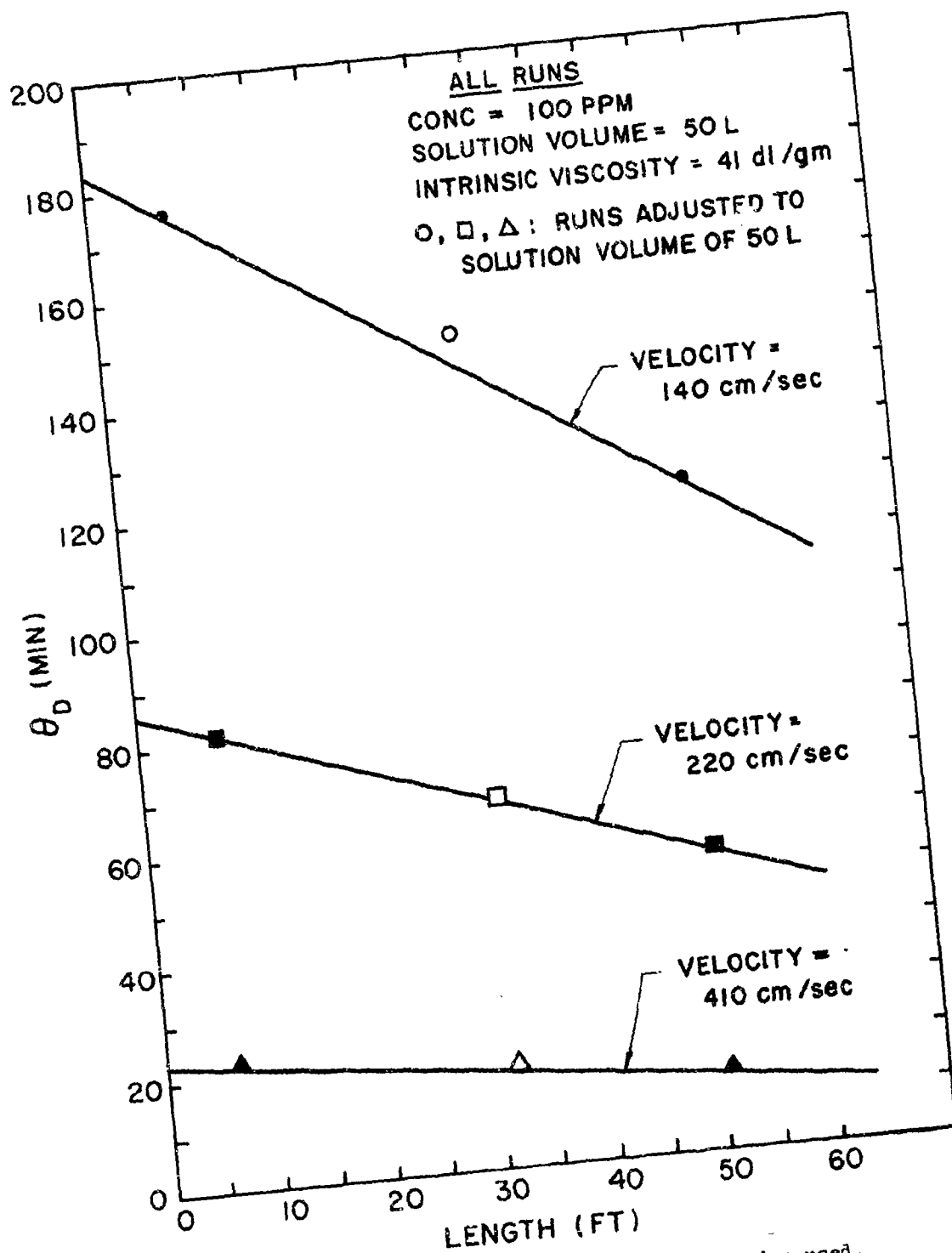
FIG. 6. Percent drag reduction-time plot for various polymer concentrations at various velocities.

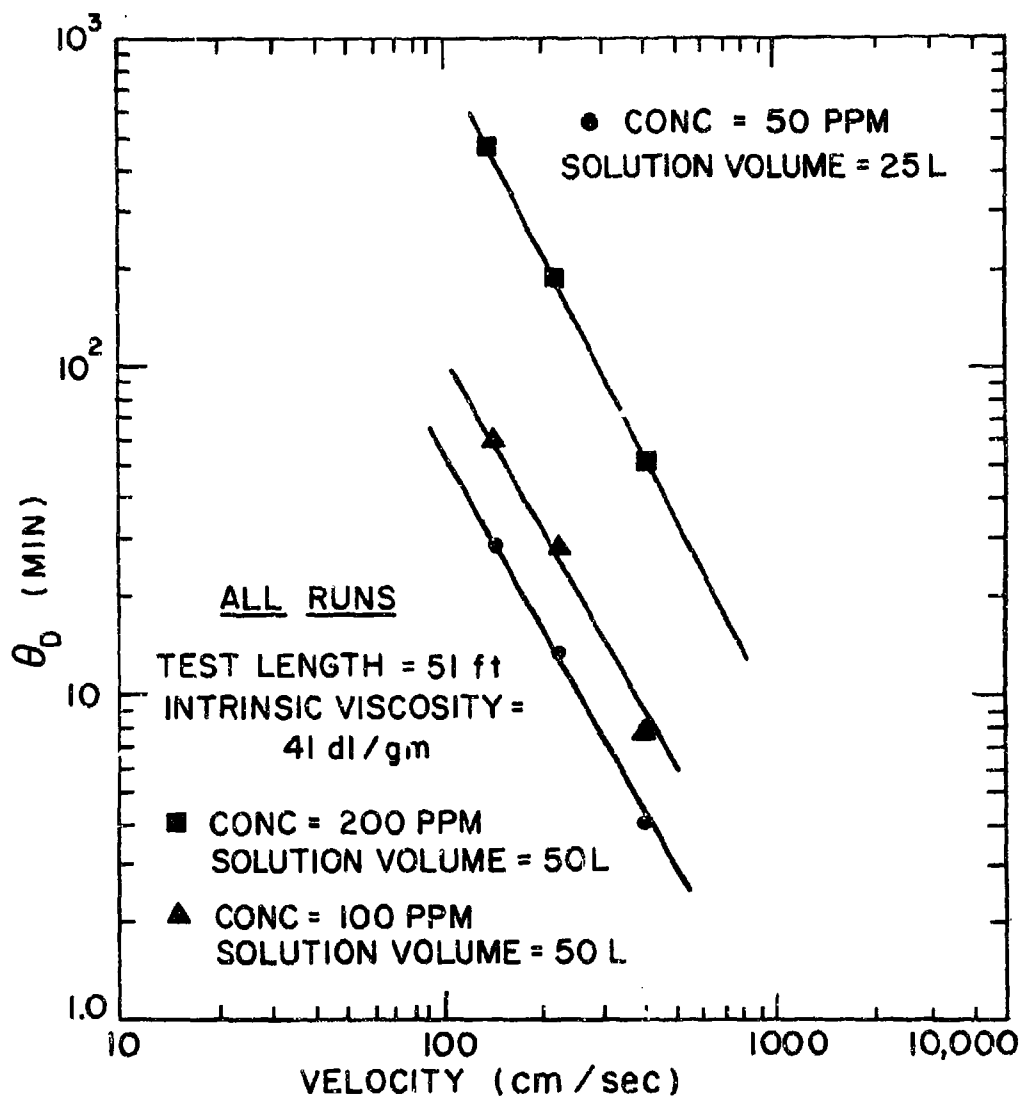
- c) Flow velocity.
- d) Polymer concentration.
- e) Intrinsic viscosity of polymer solution.

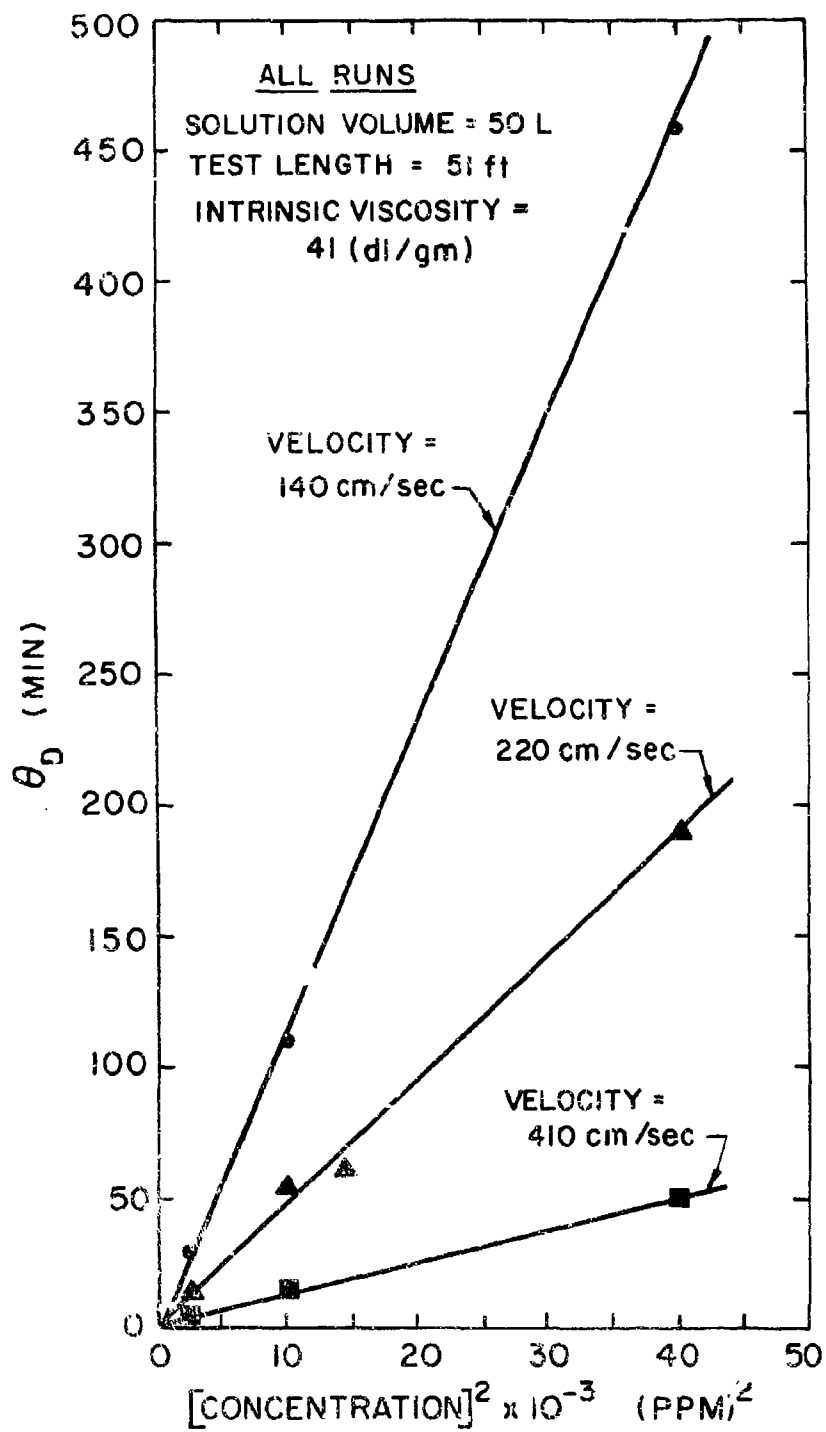
Each variable was treated independently, that is, while holding the others constant, and will be discussed in order. Our object here is to relate  $\theta_D$  and  $\theta_E$  to the variables listed such that the effect of the pump and solution volume tested can be eliminated permitting the determination of new quantities  $\theta'_D$  and  $\theta'_E$  which can be related directly to the variables of primary interest - velocity, concentration, and intrinsic viscosity. Figure 7 shows that  $\theta_D$  is proportional to the volume of the solution tested. Figure 8 shows that  $\theta_D$  is a linear function of the length of the flow section including the pump. Extrapolation of  $\theta_D$  versus length lines to zero tube length permitted the determination of the degradation effect of the pump in terms of an equivalent length of tubing (see Appendix A). Figure 9 shows that  $\theta_D$  is inversely proportional to the velocity squared and Figure 10 that  $\theta_D$  is directly proportional to the polymer concentration squared. Figure 11 shows that  $\theta_D$  is proportional to the intrinsic viscosity raised to  $3/2$  power. The functional dependence of  $\theta_E$  on the variables plotted in Figures 7 through 11 was the same as that for  $\theta_D$ ; however, there was more scatter in the data due to the uncertainty of the extrapolation necessary to obtain  $\theta_E$  values.

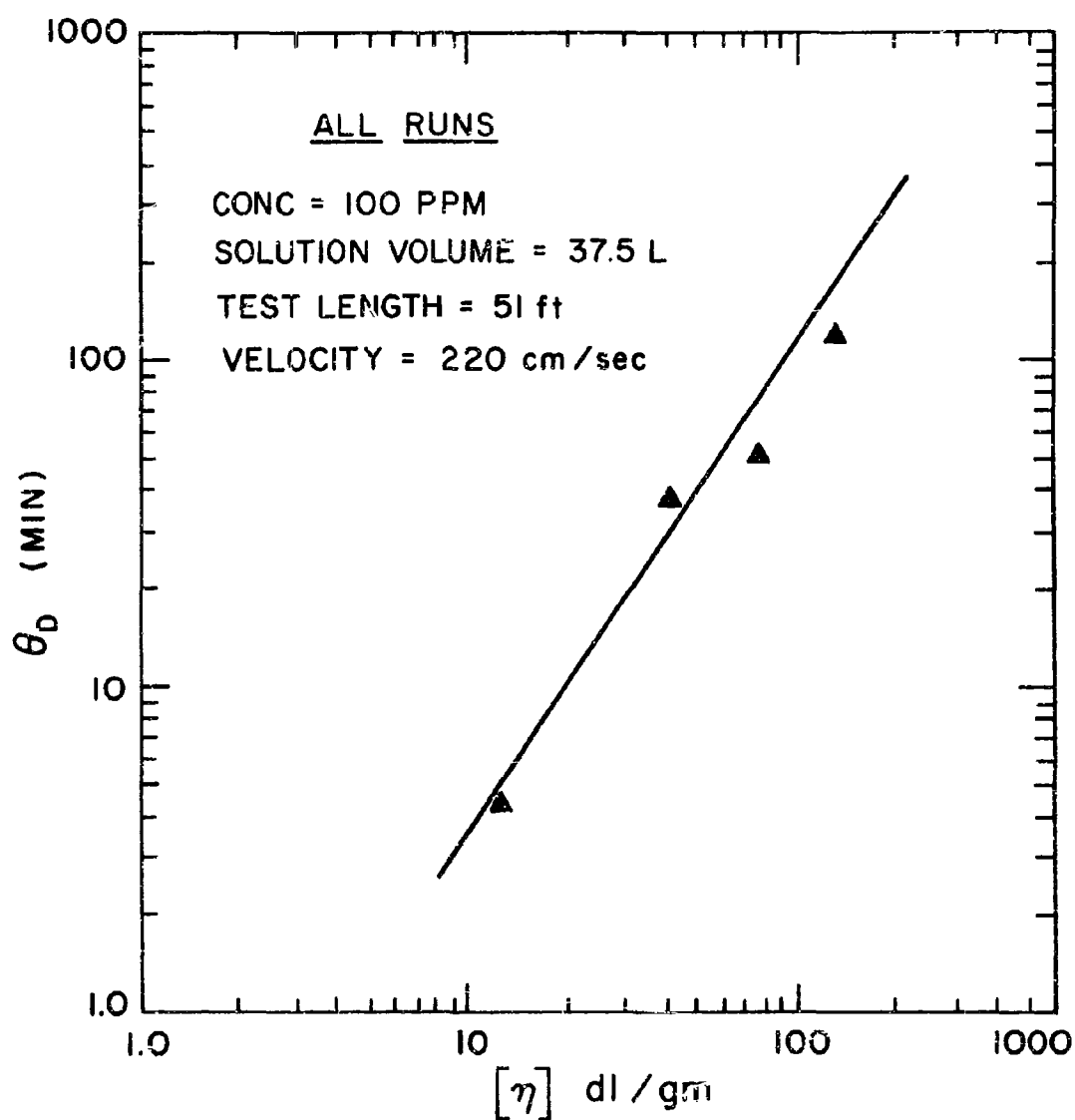
In the correlation of the experimental data, it is assumed that degradation in the feed tank and in solution preparation are negligible. The correlations to be presented are limited to the range of variables studied; i.e.

FIG. 7.  $\theta_D$  versus solution volume tested.

FIG. 8.  $\theta_D$  versus length of flow section used.

FIG. 9.  $\theta_D$  versus flow velocity.

FIG. 10.  $\theta_D$  versus polymer concentration.

FIG. 11.  $\theta_D$  versus intrinsic viscosity.



1. Polymer: Separan AP30
2. Tube Diameter: 0.244" I.D.
3. Velocity: 140-410 cm/sec, corresponding to a solvent Reynolds number, range of 10,500 - 31,000.
4. Polymer Concentration: 50-200 WPPM.
5. Intrinsic Viscosity: 12-132 dl/gm

Further experimental work is required for this polymer over a larger range of variables and especially for different tube diameters. Although it is expected that  $\theta_D$  will depend on tube diameter, the dependence may be small as it is in drag reduction (6,16,27,75-77) provided the degradation phenomena also occurs in the buffer zone. However, if degradation occurs throughout the tube cross section, a substantial diameter dependency could result. Additional work is also required for different polymers (e.g. poly(ethylene oxide)). Our preliminary work showed Polyox to be much more sensitive to drag reduction degradation than Separan which is in accord with the findings of Kenis (9) and Fisher and Rodriguez (33).

As indicated by the results shown in Figures 7 through 11, the correlation of  $\theta_D$  or  $\theta_E$  can be written in the form

$$\theta_D \propto \frac{(V_{Sol})(C)^2[\eta]^{3/2}}{(V^2)(EFF Vol_{sys})} \quad (7)$$

where

$V_{Sol}$  = Volume of Solution ( $cm^3$ )

$C$  = Polymer Concentration (gm/dl)

$[\eta]$  = Intrinsic Viscosity (dl/gm)

$V$  = Flow Velocity (cm/sec)

$EFF Vol_{sys}$  = Effective Volume of Test Section Including Pump.

and Equation (7) can be written in the form

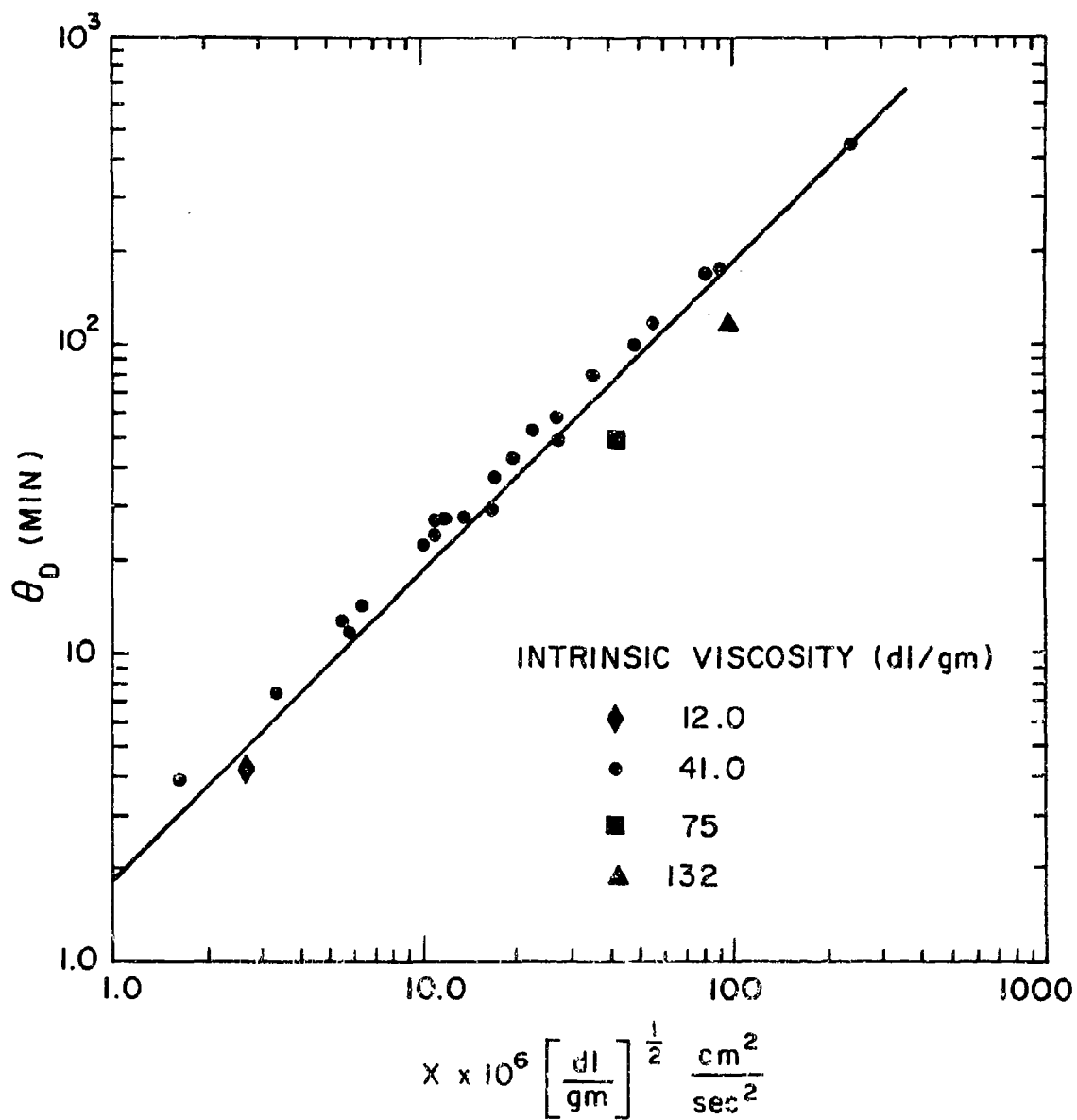
$$\theta_D = K_D X \quad (8)$$

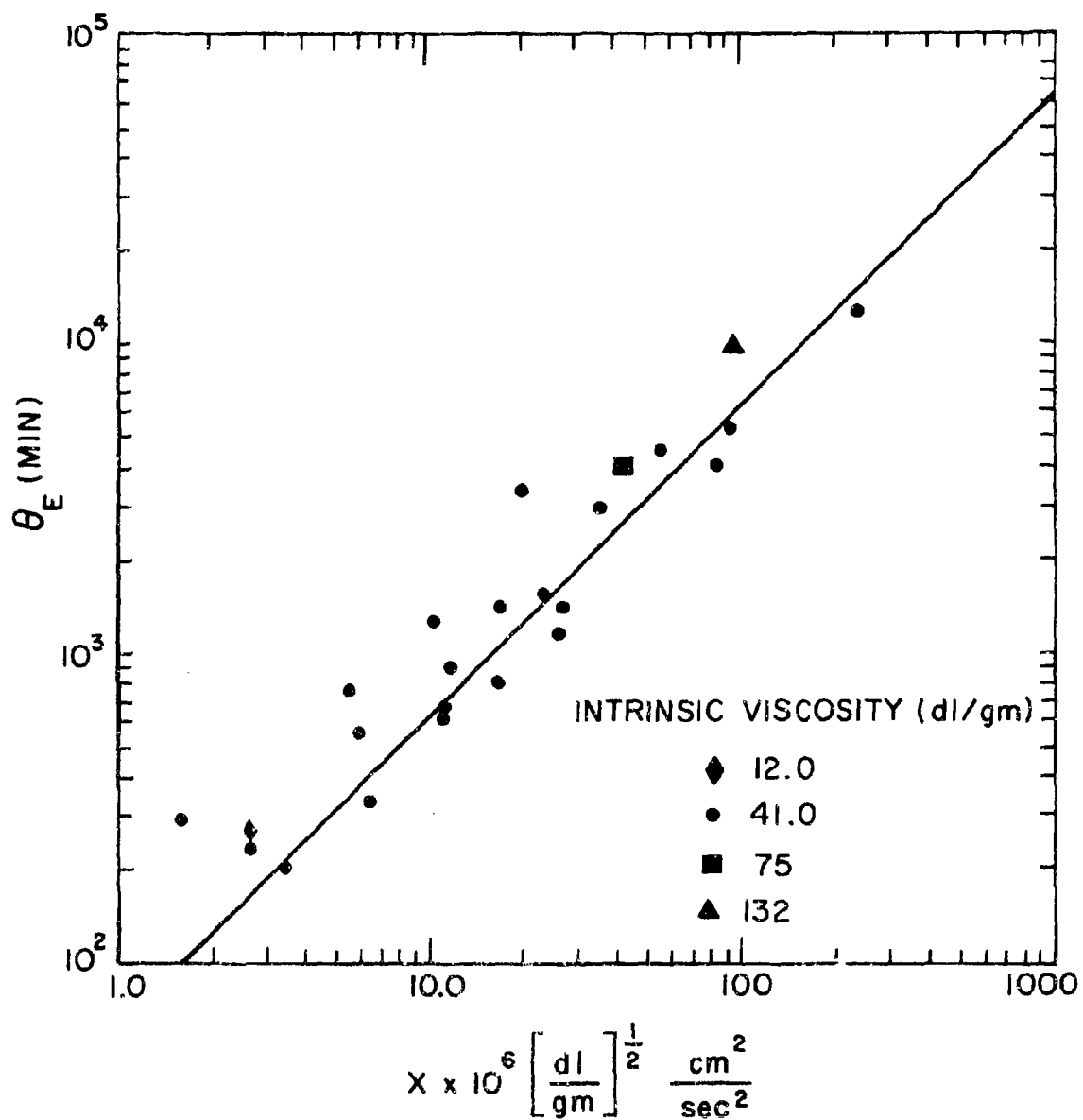
A log-log plot of  $\theta_D$  versus  $X$  should be linear with a slope of unity and is as shown in Figure 12. The average percent deviation of the data in Figure 12 is  $\pm 17\%$  and the value of  $K_D$  is  $1.87 \times 10^{-6} \frac{(\text{min})\text{cm}^2}{\text{sec}^2} \left(\frac{\text{dl}}{\text{gm}}\right)^{1/2}$

It can be seen from the correlation presented in Figure 12 that the data points for the solutions having intrinsic viscosities different from 41(dl/gm) deviate considerably from the best line through the data. Assuming that this deviation is not the result of a different dependence on the variables of Equation (7) (whose proof requires additional experimentation), the following two explanations seem reasonable. The uncertainty of the  $[\eta]$  value obtained by extrapolation of the reduced viscosity-concentration data to zero concentration for high intrinsic viscosities (e.g.  $[\eta] > 25$ ), which has been discussed in a previous study (71), may lead to  $[\eta]$  values higher than the actual values consequently yielding high values for the correlation variable,  $X$ . Also, the probability of ionic contamination of the polymer solutions in the flow system would result in effective  $[\eta]$  values lower than those measured for the pure systems again resulting in a high value for the correlation variable. Both of these effects would produce the type of deviation shown in Figure 12, especially for the two points with  $[\eta]$  values greater than 41.0. The correlation of  $\theta_E$  is given by Equation (9) and shown in Figure 13.

$$\theta_E = K_E X \quad (9)$$

The fit of  $\theta_E$  data is not as good having an average percent deviation of

FIG. 12.  $\theta_D$  versus  $X$  plot for all polymer solutions tested.

FIG. 13.  $\theta_E$  versus X plot for all polymer solutions tested.

$\pm 47.6\%$ . This is to be expected because of the uncertainty of the extrapolation necessary to obtain the  $\theta_E$  values. The value of  $K_E$  is

$62.3 \times 10^{-6} \frac{\text{min cm}^2}{\text{sec}^2} \left( \frac{\text{dl}}{\text{gm}} \right)^{1/2}$ . The  $\theta_E$  values are more than an order of magnitude greater than  $\theta_D$ .

Since both  $\theta_D$  and  $\theta_E$  depend on the solution volume and the particular pump used, it is desirable to eliminate these effects and thus determine the quantities  $\theta'_D$  and  $\theta'_E$  which are dependent only on the primary variables of interest - velocity, concentration, and intrinsic viscosity. The required relations are

$$\theta'_D = K'_D Y \quad (10)$$

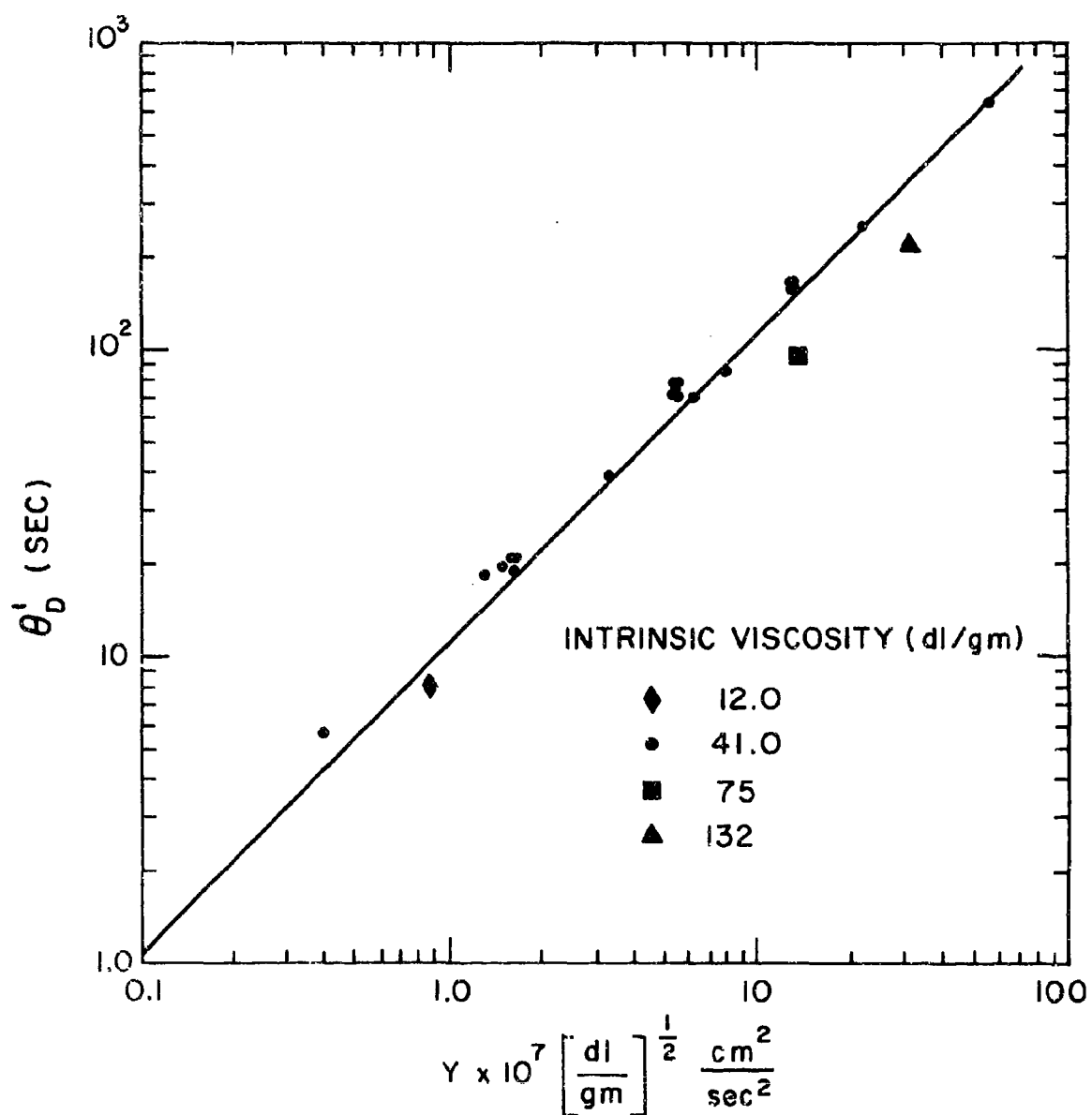
$$\theta'_E = K'_E Y \quad (11)$$

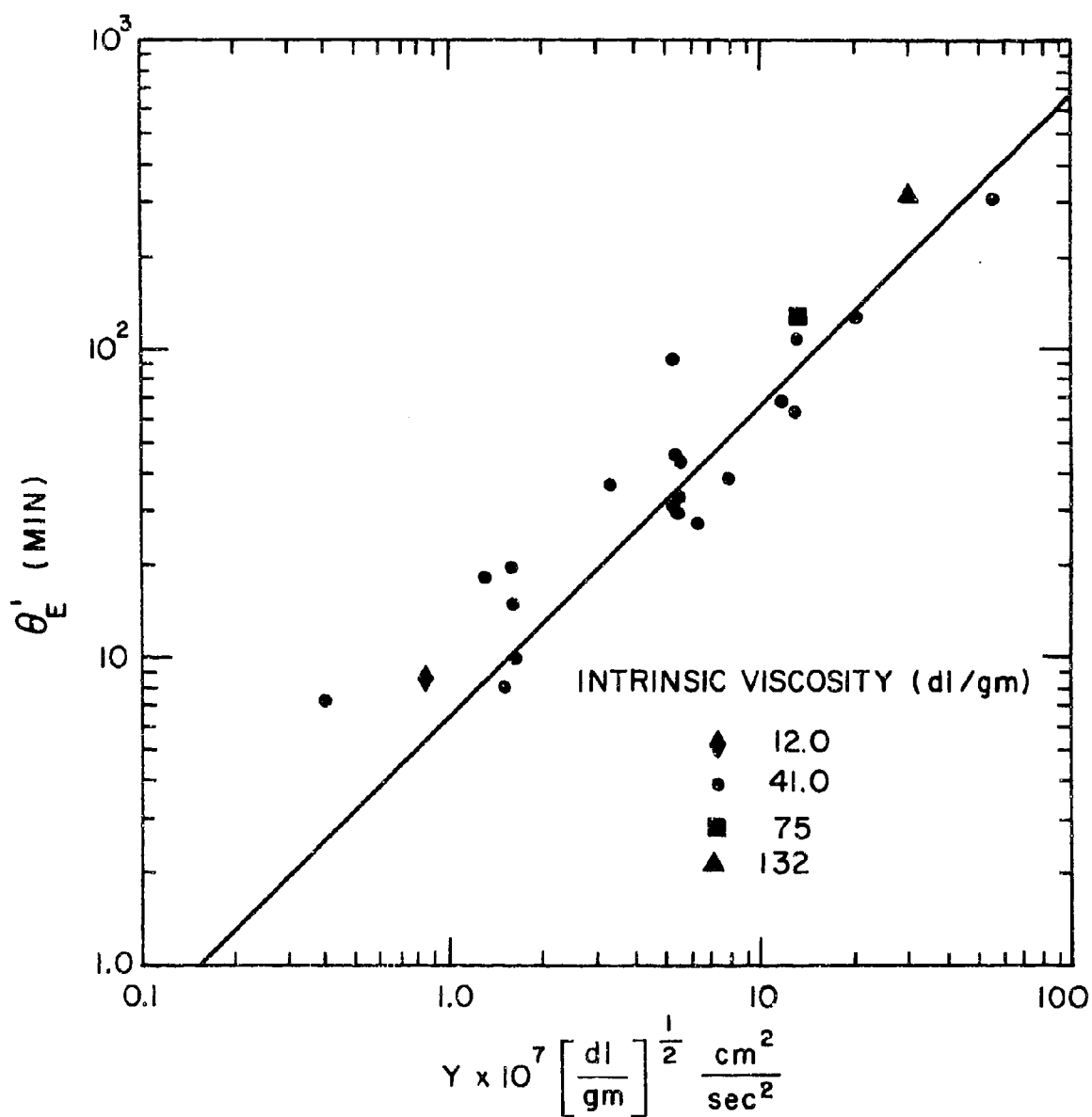
where

$$Y = \frac{C^2 [\eta]^{3/2}}{V^2} \quad (12)$$

and the data are shown in Figures 14 and 15. The average percent deviation of  $\theta'_D$  is  $\pm 19.4\%$  and that of  $\theta'_E$   $\pm 44\%$ .  $K'_D$  was found to be  $10.92 \times 10^{-7} \frac{\text{cm}^2}{\text{sec}} \left( \frac{\text{dl}}{\text{gm}} \right)^{1/2}$  and  $K'_E$  was  $6.6 \times 10^{-7} \frac{\text{min cm}^2}{\text{sec}^2} \left( \frac{\text{dl}}{\text{gm}} \right)^{1/2}$

For the range of variables studied, the correlation presented can be used as follows. For a given polymer solution (concentration and intrinsic viscosity known) under specific flow conditions (average velocity known) the variable  $Y$  can be calculated from Equation (12). With  $Y$  known  $\theta'_D$  and  $\theta'_E$  can be determined from Figures 14 and 15 or Equations 10 and 11 respectively.  $\theta'_D$  gives the real time maximum drag reduction will exist

FIG. 14.  $\theta'_D$  versus  $Y$  plot for all polymer solutions.

FIG. 15.  $\theta'_E$  versus  $Y$  plot for all polymer solutions.

while  $\theta'_E$  gives the real time that significant drag reduction (approximately 20%) will last. Both quantities  $\theta'_D$  and  $\theta'_E$  are for polymer solutions continuously being sheared in turbulent flow.



### Conclusions and Recommendations

Many papers (1-10) have appeared showing the spectacular effects that polymers can achieve in reducing frictional drag for turbulent pipe flow. These papers point out the elaborate precautions taken in order to avoid polymer solution degradation. Before drag reducing polymers can be utilized intelligently, the drag reduction degradation characteristics of these polymers must be understood. Several papers (30,34) have presented degradation data of polymer solutions; however, the data reported were exclusively on molecular degradation. Recently, attempts have been made to relate molecular degradation of these polymers to drag reduction degradation (9,10,33).

In this study, the drag reduction degradation characteristics of Separan AP30 have been reported and a limited amount of success has been achieved in relating the degradation characteristics of Separan AP30 to polymeric, system, and flow variables.

Using a recycle pressure drop experiment, pressure gradients and flow rate measurements were taken at specific intervals of time. From this data, friction factor - time plots were constructed. All friction factor-time plots on log-log coordinates exhibited three distinct regions:

- 1) At short times, a constant friction factor given by Virk's equation.
- 2) A linear region in which the friction factor increases with time for time greater than  $\theta_D$ .
- 3) At long times, an asymptotic nonlinear approach of the polymer solution friction factor toward the solvent friction factor.

From these plots,  $\theta_D$ , the process time maximum drag reduction existed, was determined from the intersection of the straight line extrapolations of regions one and two. Likewise,  $\theta_E$ , the process time significant drag reduction existed ( $20 \pm 5\%$ ), was determined from the intersection of straight line extrapolations of region two and the solvent friction factor.

For the limited range of the variables listed below:

- 1) Polymer: Separan AP30
- 2) Concentration: 50-200 PPM
- 3) Velocity: 140-410 cm/sec
- 4) Intrinsic Viscosity: 12-132 dl/gm
- 5) Tube Diameter: 0.619 cm
- 6) Test Section Length: 213-1550 cm
- 7) Volume of Solution Tested: 25-50 liters

Correlations are presented relating  $\theta_D$  and  $\theta_E$  to these variables and are given by equations (3) and (9) respectively.

$$\theta_D = 1.87 \times 10^{-6} X \quad (8)$$

$$\theta_E = 62.3 \times 10^{-6} X \quad (9)$$

where X is defined by equation (7).

Correlations are also presented which relate the drag reduction characteristics of Separan AP30 to the variables of primary interest - intrinsic viscosity, concentration, and velocity.  $\theta'_D$ , the real time maximum drag reduction exists for a solution under continuous shearing conditions, is related to these variables by equation (10)

$$\theta'_D = 10.92 \times 10^{-7} Y \quad (10)$$

where  $\gamma$  is defined by equation (12).  $\theta'_E$ , the real time significant drag reduction exists ( $20 \pm 5\%$ ) for a solution under continuous shearing conditions, is also related to these variables and is given by equation (11).

$$\theta'_E = 6.6 \times 10^{-7} \gamma \quad (11)$$

Two limitations severely restrict the use of these correlations; the most important being the fact that they are for a single tube diameter (0.619 cm); secondly that they are for a single polymer, Separan AP30. Therefore, it is recommended that the range of all variables be extended, especially tube diameter and polymer type. Ideally, an experimental study should have the capability of continuously monitoring the composition and molecular weight distribution of the polymer solution during shear. Thus although the correlations presented are limited, it is believed that the essential drag-reduction degradation behavior of dilute polymer solutions in turbulent flow has been demonstrated and that the ideas and results presented should stimulate additional research which will further elucidate this highly complex and important phenomena.

Bibliography

1. B. A. Toms, Proc. 1st. Int. Congress on Rheology, Vol. 2, 135 (1948); North Holland.
2. C. S. Wells, Editor, Viscous Drag Reduction (1969); Plenum Publishing Company.
3. E. R. Van Driest, J. of Hydronautics, 4(3), 120 (1970).
4. J. G. Savins, Soc. Petrol. Engng. J., 4, 203 (1964).
5. C. Elata, J. Lehrer, and A. Kahanovitz, Israel J. Technol., 4, 87 (1966).
6. F. A. Seyer and A. B. Metzner, A.I.Ch.E. J., 15, 426 (1969).
7. P. S. Virk, J. Fluid Mech., 45(3), 417 (1971).
8. G.-C. Liaw, J. L. Zakin, and G. K. Patterson, A.I.Ch.E. J., 17(2), 391 (1971).
9. P. R. Kenis, J. Appl. Poly. Sci., 15, 607 (1971).
10. R. W. Paterson and F. H. Abernathy, J. Fluid. Mech., 43(4), 689 (1970).
11. G. K. Patterson, J. L. Zakin and J. M. Rodriguez, Ind. Eng. Chem., 61(1), 22 (1969).
12. J. L. Lumley, Annual Rev. Fluid Mech., 1, 367 (1969), Annual Reviews Inc., Palo Alto, Calif.
13. A. Peterlin, Nature, 227, 598 (1970).
14. R. J. Gordon, J. Appl. Poly. Sci., 14, 2097 (1970).
15. G. Astarita, Ind. Eng. Chem. Fundam., 4, 354 (1965).
16. G. Astarita, G. Greco, and L. Nicodemo, A.I.Ch.E. J., 15, 564 (1969).
17. H. C. Hershey and J. L. Zakin, Chem. Eng. Sci., 22, 1847 (1967).
18. W. A. Meyer, A.I.Ch.E. J., 12, 522 (1966).
19. G. K. Patterson and J. L. Zakin, A.I.Ch.E. J., 14, 434 (1968).
20. S. J. Kline, W. D. Reynolds, F. A. Schraub, and P. W. Runstadler, J. Fluid Mech., 30, 741 (1967).
21. J. Laufer, N.A.C.A. Rep. 1174 (1954).
22. P. S. Klebanoff, N.A.C.A. Rep. 1247 (1955).
23. J. O. Hinze, Turbulence, McGraw-Hill, New York; (1959).

Bibliography (continued)

24. H. P. Bakewell and J. L. Lumley, *Phys. Fluids*, 10, 1880 (1967).
25. E. E. Corino and R. S. Brodkey, *J. Fluid Mech.*, 37, 1 (1969).
26. A. G. Fabula, *Proc. 4th Int. Congress on Rheology, Part 3*, pp. 455-479 Interscience; (1965).
27. P. S. Virk, E. W. Merrill, H. S. Mickley and E. L. Mollo-Christensen, *J. Fluid Mech.*, 30, 305 (1967).
28. E. W. Merrill, K. A. Smith, H. Shin, and H. S. Mickley, *Trans. Soc. Rheol.*, 10, 335 (1966).
29. M. E. LePera and J. Pigliacampi, *Ind. Eng. Chem. Prod. Res. Develop.*, 9, 525 (1970).
30. A. Ram and A. Kadim, *J. Appl. Polym. Sci.*, 14, 2145 (1970).
31. W. R. Johnson and C. C. Price, *J. Polym. Sci.*, 45, 217 (1960).
32. E. W. Merrill, H. S. Mickley, and A. Ram, *J. Polym. Sci.*, 62, S109 (1962).
33. D. H. Fisher and F. Rodriguez, Degradation of Drag-Reducing Polymers, Paper presented at the 69th Nat. Meeting of American Institute of Chemical Engineers, May 16-19 (1971), Cincinnati, Ohio.
34. D. A. White, *Chem. Engr. Sci.*, 25, 1255 (1970).
35. A. Nakano and Y. Minoura, *J. Appl. Poly. Sci.*, 15, 927 (1971).
36. Y. Minoura, T. Kasuya, S. Kawamura, and A. Nakano, *J. Polym. Sci.*, A-1, 5, 45; A-2, 5, 125 (1967).
37. D. W. Ovenall, G. W. Hastings, and P.E.M. Allen, *J. Polym. Sci.*, 33, 207 (1958).
38. D. W. Ovenall, *J. Polym. Sci.*, 42, 455 (1960).
39. H. H. G. Jellinek and G. White, *J. Polym. Sci.*, 6, 745, 759 (1951); *ibid.* 7, 21, 33 (1952).
40. H. Fujiwara and K. Goto, *J. Chem. Soc., Japan, Ind. Chem. Soc.*, 71, 1430 (1968).
41. K. Arai, K. Nakamura, T. Komatsu, and T. Nakagawa, *ibid.*, 71, 1438 (1968).
42. H. Grohn and G. Opitz, *Plaste und Kaut.*, 11, 11 (1964).
43. R. E. Harrington, *J. Polym. Sci.*, A-1, 4, 489 (1966).
44. F. Rodriguez and C. C. Winding, *Ind. Eng. Chem.*, 51, 1281 (1959).

Bibliography (continued)

45. R. S. Porter, M.J.R. Cantow, and J. F. Johnson, J. Appl. Phys., 35, 15 (1964).
46. H.H.G. Jellinek, Degradation of Vinyl Polymers, Academic Press, Inc., New York (1955).
47. P. Alexander and M. Fox, J. Polym. Sci., 12, 533 (1954).
48. G. Schmid, G. Paret, and H. Pffeiderer, Kolloid-Z, 124, 150 (1951).
49. H. W. Melville and A.J.R. Murray, Trans. Faraday Soc., 46, 996 (1950).
50. M. T. Shaw and F. Rodriguez, J. Appl. Poly. Sci., 11, 991 (1967).
51. G. Gooberman and J. Lamb, J. Polym. Sci., 42, 35 (1960).
52. M.A.K. Mostofa, J. Polym. Sci., 33, 311 (1958).
53. A. Weissler, J. Appl. Phys., 21, 171 (1950).
54. G. K. Patterson, H. C. Hershey, C. D. Green and J. L. Zakin, Trans. Soc. Rheol., 10(2), 489 (1966).
55. G. Gooberman, J. Polym. Sci., 42, 25 (1960).
56. F. Bueche, J. Appl. Poly. Sci., 4, 101 (1960).
57. A. B. Bestul, J. Chem. Phys., 32, 350 (1960).
58. I.R.M. Gail and A. L. Neville, J. Inst. Petrol., 55, 542 (1969).
59. A. Ram and A. Tamir, J. Appl. Poly. Sci., 8, 2751 (1964).
60. T. D. Foster and R. R. Mueller, ASTM Pub., 382, 14 (1964).
61. E. E. Klaus, E.J. Tewksbury, R. M. Jolie, W. A. Lloyd and R. E. Manning, ASTM Pub. 382, 45 (1964).
62. T. W. Selby, ASTM Pub. 382, 58 (1964).
63. G. K. Vick and R. M. Goodson, ASTM Pub., 382, 33 (1964).
64. A. Ram, in Rheology, Vol. 4, E. R. Eirich, Ed., Academic Press, New York. (1967).
65. W. L. Hawkins and F. H. Winslow, in Chemical Reactions of Polymers pp. 1055-1083, E. M. Fettes, Ed., Interscience, New York (1964).
66. J. Furukawa and T. Saegusa, Polymerization of Aldehydes and Oxides, Interscience, New York (1963).

Bibliography (continued)

67. F. Rodriguez, Principles of Polymer Systems, pp. 270-297, McGraw-Hill, New York (1970).
68. R. H. Mellen, J. Acoust. Soc. Am. 28, 447 (1956).
69. B. B. Thomas and W. J. Alexander, J. Polym. Sci., 15, 361 (1955).
70. K. Goto and H. Fujiwara, Kobunshi Kagaku, 21, 716 (1964).
71. N. D. Sylvester and J. S. Tyler, Ind. Engr. Chem. Prod. Develop. 9, 548 (1970).
72. P. J. Flory, Principles of Polymer Chemistry, Cornell Univ. Press, Ithaca, N. Y. (1953).
73. M. L. Huggins, Physical Chemistry of High Polymers, J. Wiley & Sons, New York (1958).
74. R. Stromberg, A.F.M. Lab. Tech. Dept. AFML-TR-65-276 (1966).
75. J. M. Rodriguez, J. L. Zakin and G. K. Patterson, Soc. Pet. Eng. J. 7, 325 (1967).
76. G. K. Patterson, J. L. Zakin and J. M. Rodriguez, A.I.Ch.E. J., 16, 505 (1970).
77. F. A. Seyer and A. B. Metzner, Can. J. Chem. Engr., 47, 525 (1969).

Appendix A

If the pump had no degradation effect on the polymer solutions, then  $\theta_D$  should approach infinity as  $L$  approached zero; however, this was not the case as can be seen in Figure 8. Therefore,  $\theta_D$  must be inversely proportional to the length of the test section,  $L$ , plus an additional length which accounts for the degradation effect of the pump,  $L'$ .

$$\theta_D \propto \frac{1}{L+L'} \quad (A-1)$$

Since the curves shown in Figure 8 are linear, the ratio given in equation (A-2) can be found from any two points on a constant velocity line.

$$\frac{\theta_D^{(1)}}{\theta_D^{(2)}} = \frac{L^{(2)} + L'}{L^{(1)} + L'} \quad (A-2)$$

$L'$  is assumed at this point to be constant for a given pump rotational speed. Solving for  $L'$  in equation (A-2), we obtain

$$L' = \frac{\theta_D^{(2)} L^{(2)} - \theta_D^{(1)} L^{(1)}}{\theta_D^{(1)} - \theta_D^{(2)}} \quad (A-3)$$

Using equation (A-3), the value of  $L'$  was calculated for each value of the flow velocity. All three values of  $L'$  were found to be approximately equal to  $2300 \pm 200$  cm. The average value (2324 cm) was used to calculate the effective volume of the test section.

$$\text{EFF Vol}_{\text{sys}} = \frac{\pi D^2}{4} (L + L') \quad (A-4)$$



Therefore, the additional degradation effect caused by increasing the pump rotational speed to achieve higher flow rates was accounted for completely by the velocity term in Equation (7).

TABLE AI  
SUMMARY OF THE SEPARAN-AP30 DRAG REDUCTION DEGRADATION DATA

Run No.	$Q_D$ (ml/min)	Velocity (cm/sec)	Solvent $N_{He}$	Conc (gm/dl)	Solution Volume (cm <sup>3</sup> )	EFF System Volume (cm <sup>3</sup> )	Intrinsic Viscosity (dl/gm)	$\gamma \cdot 10^{-6}$	$Q_D'$ (sec)	$Q_E$ (min)	$Q_E'$ (min)
1	25.0	223.23	17,186	0.01	25,000	1170.04	41.0	5.2664	70.202	680.0	31.825
2	60.0	143.57	11,030	0.01	25,000	1170.04	41.0	12.7364	168.486	1450.0	67.862
3	28.0	221.50	17,017	0.01	25,000	1170.04	41.0	5.3509	78.627	640.0	29.953
4	7.6	404.28	31,059	0.01	25,000	1170.04	41.0	3.432	21.342	210.0	9.828
5	28.0	217.51	16,710	0.01	25,000	1170.04	41.0	5.5490	78.627	920.0	43.057
6	30.0	218.83	16,812	0.012	25,000	1170.04	41.0	16.869	84.243	820.0	38.379
7	54.0	221.22	16,995	0.01	50,000	1170.04	41.0	5.3645	75.819	1450.0	33.931
8	82.0	218.	16,803	0.01	50,000	765.54	41.0	5.4878	329	3000.0	45.932
9	175.0	141.88	10,900	0.01	50,000	765.54	41.0	85.181	160.763	4100.0	62.774
10	23.0	402.21	30,900	0.01	50,000	765.54	41.0	1.6228	21.129	1300.0	19.904
11	13.0	223.88	17,200	0.005	50,000	1170.04	41.0	5.597	18.253	770.0	18.019
12	180.0	220.68	16,954	0.02	50,000	1170.04	41.0	21.5630	252.729	5500.0	128.704
13	4.0	410.71	31,553	0.005	50,000	1170.04	41.0	0.3991	5.616	300.0	7.020
14	50.0	410.53	31,539	0.02	50,000	1170.04	41.0	6.2308	70.202	1175.0	27.486
15	28.0	140.94	10,828	0.005	50,000	1170.04	41.0	3.3040	39.313	1550.0	36.271

TABLE AI (continued)

Run No.	$\theta_D$ (min)	Velocity (cm/sec)	Solvent $n_D$	Conc (gm,dl)	Solution Volume (cm <sup>3</sup> )	EFF System Volume (cm <sup>3</sup> )	Efficiency (%)	$X \cdot 10^6$	$Y \cdot 10^7$	$\theta'_2$ (sec)	$\theta_2$ (min)	$\theta'_2$ (min)
16	460.0	137.02	10,527	0.02	50,000	1170.04	41.0	239.022	55.9330	645.862	13,000.0	304.210
17	14.5	415.20	31,898	0.01	50,000	1170.04	41.0	6.503	1.5229	20.359	340.0	7.956
18	120.0	142.09	10,916	0.01	50,000	1170.04	41.0	55.567	13.0032	163.486	4600.0	107.644
19	38.0	220.90	16,971	0.01	37,500	1170.04	41.0	17.244	5.3800	71.138	1450.0	45.241
20	118.0	223.09	17,139	0.01	37,500	1170.04	132.0	97.664	30.4720	220.904	10,000	312.011
21	4.5	221.23	16,996	0.01	37,500	1170.04	12.0	2.722	0.8493	8.424	275	8.590
22	44.0	221.88	17,046	0.01	37,500	995.37	41.0	20.092	5.3326	70.074	3400	90.247
23	12.0	403.46	30,996	0.01	37,500	995.37	41.0	6.077	1.6128	19.111	560	14.864
24	100.0	142.28	10,931	0.01	37,500	995.37	41.0	48.857	12.9684	159.259	29,500	783.024
25	50.0	219.67	16,876	0.01	37,500	1170.04	75.0	43.141	13.4602	93.603	4,000	124.804